

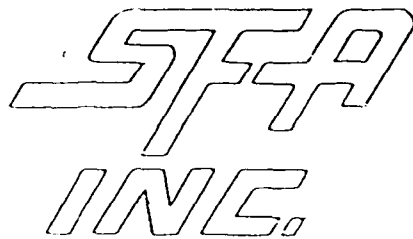


DTIC FILE COPY

AD-A228 749

S D T I C  
ELECTED  
NOV 16 1990  
S E D

DISTRIBUTION STATEMENT A  
Approved for public release  
Distribution Unlimited



## FINAL REPORT

### INVESTIGATION AND MODELING OF RADIATION ABSORPTION PROCESSES AND OPACITIES IN DENSE PLASMAS

1990

FOR AIR FORCE OFFICE OF SCIENTIFIC RESEARCH

2  
DTIC  
ELECTED  
NOV 16 1990  
S E D

---

1401 MCCORMICK DRIVE, LANDOVER, MARYLAND 20785  
(301) 925-9400

DISTRIBUTION STATEMENT A

Approved for public release;  
Distribution Unlimited

## REPORT DOCUMENTATION PAGE

Form Approved  
OMB No. 0704-0188

1. REPORT SECURITY CLASSIFICATION U UNCLASSIFIED		1b. RESTRICTIVE MARKINGS										
2. SECURITY CLASSIFICATION AUTHORITY		3. DISTRIBUTION/AVAILABILITY OF REPORT Distribution Unlimited; <i>Approved for public release.</i>										
3. DECLASSIFICATION/DOWNGRADING SCHEDULE												
4. FORMING ORGANIZATION REPORT NUMBER(S) FA-0184Z		5. MONITORING ORGANIZATION REPORT NUMBER(S) AFOSR-TR- 90 1073										
6. NAME OF PERFORMING ORGANIZATION FA, Inc.	6b. OFFICE SYMBOL (If applicable)	7a. NAME OF MONITORING ORGANIZATION AFOSR/NP										
7. ADDRESS (City, State, and ZIP Code) 401 McCormick Drive andover, MD 20785		7b. ADDRESS (City, State, and ZIP Code) Building 410 Bolling AFB DC 20332-6448										
8. NAME OF FUNDING/SPONSORING ORGANIZATION AIR FORCE CENTRE OF SCIENTIFIC RESEARCH	8b. OFFICE SYMBOL (If applicable) NP	9. PROCUREMENT INSTRUMENT IDENTIFICATION NUMBER F49620-88-C-0055										
10. ADDRESS (City, State, and ZIP Code) BUILDING 410, BOLLING AFB D.C. 20332-6448		10. SOURCE OF FUNDING NUMBERS <table border="1"><tr><td>PROGRAM ELEMENT NO. 61102F</td><td>PROJECT NO. 2301</td><td>TASK NO. A8</td><td>WORK UNIT ACCESSION NO.</td></tr></table>		PROGRAM ELEMENT NO. 61102F	PROJECT NO. 2301	TASK NO. A8	WORK UNIT ACCESSION NO.					
PROGRAM ELEMENT NO. 61102F	PROJECT NO. 2301	TASK NO. A8	WORK UNIT ACCESSION NO.									
11. TITLE (Include Security Classification) (U) INVESTIGATION AND MODELING RADIATION ABSORPTION PROCESSES AND OPACITIES IN DENSE PLASMAS												
12. PERSONAL AUTHOR(S) day Gupta, PhD												
13. TYPE OF REPORT FINAL	13b. TIME COVERED FROM 04/01/88 TO 02/28/90	14. DATE OF REPORT (Year, Month, Day) 1990	15. PAGE COUNT 101									
16. SUPPLEMENTARY NOTATION												
17. COSATI CODES <table border="1"><tr><th>FIELD</th><th>GROUP</th><th>SUB-GROUP</th></tr><tr><td>6.1</td><td></td><td></td></tr><tr><td>6.3</td><td></td><td></td></tr></table>		FIELD	GROUP	SUB-GROUP	6.1			6.3			18. SUBJECT TERMS (Continue on reverse if necessary and identify by block number) <i>Dense Plasma Plasma Opacities</i> <i>Ionic Species</i>	
FIELD	GROUP	SUB-GROUP										
6.1												
6.3												
19. ABSTRACT (Continue on reverse if necessary and identify by block number) <p>A variety of atomic processes contribute to absorption of radiation in dense plasmas. Most existing atomic data is for low density, high temperature plasmas. At high densities and low temperatures, realistic modeling to incorporate the important additional effects in order to generate atomic data is needed. This is addressed in the present work.</p> <p>The models and computer codes developed for the project includes effects of non-linear screening, electron degeneracy, exchange-correlation and ion interactions self-consistently. These were applied to ions of specific configurations in dense plasmas and represent improvements over 'average atom models' often used in dense plasma physics.</p> <p>The focus of this work is mainly on the bound-bound, bound-free and free-free photoprocesses, that contribute to ionization absorption and opacity of dense, low temperature plasmas. We discuss a model to generate ionic distribution function which is computationally faster than rate equation method. We also discuss a model to investigate the d.c. electron recombination in dense plasmas, which incorporates effects of multiple scattering and improves over the Ziman type model.</p> <p style="text-align: right;">Continue on reverse...</p>												
20. DISTRIBUTION/AVAILABILITY OF ABSTRACT UNCLASSIFIED/UNLIMITED <input checked="" type="checkbox"/> SAME AS RPT. <input type="checkbox"/> DTIC USERS		21. ABSTRACT SECURITY CLASSIFICATION										
22. NAME OF RESPONSIBLE INDIVIDUAL Robert J. Becker		22b. TELEPHONE (Include Area Code) 202-767-5011	22c. OFFICE SYMBOL NP									

SECURITY CLASSIFICATION: Unclassified

SFA-0184Z

INVESTIGATION AND MODELING OF RADIATION  
ABSORPTION PROCESSES AND OPACITIES IN DENSE  
PLASMAS

PREPARED BY:

UDAY GUPTA, PHD



SFA, INC.  
1401 McCormick Drive  
Landover, Maryland 20785

SEPTEMBER, 1990

CONTRACT NUMBER NO: F49620-88-C-0055

Accession For	
NTIS GRA&I <input checked="" type="checkbox"/>	
DTIC TAB <input type="checkbox"/>	
Unannounced <input type="checkbox"/>	
Justification _____	
By _____	
Distribution/ _____	
Availability Codes	
Dist	Avail and/or Special
A-1	

PREPARED FOR:

AIR FORCE OFFICE OF SCIENTIFIC RESEARCH  
BUILDING 410  
BOLLING AFB  
WASHINGTON, D.C. 20332-6448

---

1401 MCCORMICK DRIVE, LANDOVER, MARYLAND 20785  
(301) 925-9400

## TABLE OF CONTENTS

	Page
INTRODUCTION	1
I ATOMIC MODEL FOR IONS OF SPECIFIC CONFIGURATIONS IN PLASMAS	4
II BOUND-BOUND PHOTOPROCESS	6
III BOUND-FREE PHOTOPROCESS	8
IV FREE-FREE TRANSITIONS	8
V MODEL FOR DISTRIBUTION OF IONIC SPECIES IN PLASMAS	10
VI ELECTRICAL CONDUCTIVITY IN HOT DENSE PLASMAS	15
RESULTS	19
CONCLUSIONS	22
ACKNOWLEDGEMENTS	22
REFERENCES	23
APPENDIX I	24
FIGURE 1	
TABLES	
SAMPLE COMPUTER OUTPUT	
LISTING OF SAMPLE COMPUTER CODES: FFNEW.FOR; DIFF.FOR; SIMP.FOR; WAVEF.FOR.	

## INTRODUCTION

Modeling of radiation absorption processes in plasmas require investigation and computation of a large number of atomic processes contributing to such absorption. Bound-bound phototransition (or photoexcitation), bound-free (or photoionization) and free-free (or inverse Bremsstrahlung) photoprocess, as well as Thomson and Compton scattering of radiation and electron conduction of low energy radiation are some of these processes. This report deals with the investigation, modeling and computation of these atomic processes in plasmas.

Depending on the plasma density and temperature, several different effects need to be systematically investigated and modelled. The bulk of theoretical and experimental atomic data available in the literature is limited to isolated neutral atoms. Depending on experimental conditions, plasma ions can be ionized to a different degree of ionization. The atomic data for highly charged ions, as occur in high temperature Takamak plasmas, astrophysical plasmas<sup>1</sup> or X-ray laser plasmas are quantitatively very different from those for neutral atoms. Also, at higher plasma densities (and for comparatively lower temperatures), plasma screening effect causes ionic energy levels to shift significantly (particularly the upper levels) and modifies the effective ionic potentials so that the various atomic processes can be significantly altered. Atomic data for isolated atoms or ions are no longer valid for these dense plasma conditions. Realistic modeling of atomic processes are therefore required for dense plasmas. In addition, broadening of ionic spectral lines also occur at higher densities (such as in ICF plasmas) which influence radiation absorption processes. Line broadening is temperature sensitive as well.

At extremely high plasma densities, such as in superdense ICF pellets or in astrophysical plasmas (interior of White Dwarfs, for example), processes such as Compton scattering of radiation, as well as electron conduction of radiation becomes important for overall absorption processes and opacities. For plasmas in those conditions, these processes therefore need to be incorporated in the modeling.

The modeling and computation of radiation absorption coefficients and plasma opacities are required inputs to overall radiation hydrodynamic simulation of plasmas in a variety of laboratory and astrophysical conditions. We are concerned with low to fairly high-density plasmas as occur in laboratory discharge tube plasmas, Z-pinch plasmas, Tokamak plasmas, X-ray laser plasmas, wire-imploded plasmas, ICF and laser imploded plasmas, and for some astrophysical plasmas, such as outer layers of White Dwarfs. The atomic data for radiation absorption are essential ingredients for radiation transport simulations, as well as overall radiative (and spectroscopic) studies of plasmas in above mentioned experimental conditions.

The effect of plasma density and temperature on atomic processes has been treated in the past by 'average atom models' (AAM's).<sup>4</sup> (The Thomas-Fermi-Dirac model<sup>13,14</sup> is one of the widely used AAM's). However, there are well-known serious shortcomings of the AAM's. These models assign fractional occupation of bound electronic states and thus lead to fictitious atomic structure. The AAM's do not, therefore, generate accurate data.

For accurate calculations of atomic processes for ions in dense plasmas, the correct treatment of plasma density and temperature effects on the atomic structure of multielectron ions of specific configuration is of central importance. The specific ionic configurations with integral occupation of bound electronic states need to be considered in order to obtain realistic atomic structure. Screening by plasma electrons has to be treated in a fully non-linear fashion (since Debye-Huckel screening is known to be grossly inaccurate for dense plasmas). Screening by both bound and free electrons has to be considered in a self-consistent way. Degeneracy effect and many-electron effect such as exchange-correlation interaction need to be accounted for in the model. Depending on plasma conditions, the effect of strong-coupling (i.e. when Coulomb interaction dominates over random thermal motion) needs to be taken into account.

The main objective of the present work is to incorporate these effects systematically in the models and the relevant computer codes in order to have the capability of generating realistic atomic data for various processes

contributing to photon absorption. The bound-free (photoionization), the free-free (inverse Bremstrahlung) and the bound-bound (photoexcitation) atomic processes are of particular interest in this context. The improved models and the various computer codes would be useful tools for such calculations later on particularly for moderately high electron density range ( $\sim 10^{23}$ - $10^{24}$  e/cm<sup>3</sup>) and relatively lower temperature range ( $\sim 10$ -200 eV.....) where 'average atom' type models are known to be inadequate.

## I. ATOMIC MODEL FOR IONS OF SPECIFIC CONFIGURATIONS IN PLASMAS

For a given ion immersed in a plasma of mean electron density  $\bar{\rho}_e$  and mean ion density  $\bar{\rho}_i$  at temperature T, we have a coupled system of equations for electrons and ions to solve. For electrons, we have,

$$\left[ -\frac{1}{2} \nabla^2 + V_e(\vec{r}) \right] \phi_i(\vec{r}) = \epsilon_i \phi_i(\vec{r}) \quad I-(1)$$

with

$$V_e(\vec{r}) = -\frac{z}{r} - \int \frac{[\bar{z} \rho_i(\vec{r}') - \rho_e(\vec{r}')] }{|\vec{r} - \vec{r}'|} d\vec{r}' + V_{xc}(\vec{r}) - V_{xc}(\vec{R}), \quad I-(2)$$

$$\rho_e(\vec{r}) = \sum_b f_b |\phi_b(\vec{r})|^2 + \sum_{l=0}^{\infty} 2(2l+1) \int_0^{\infty} dk k^2 f(k) |\phi_{kl}(\vec{r})|^2, \quad I-(3)$$

and for ions

$$\rho_i(\vec{r}) = \bar{\rho}_i e^{-V_i/k_B T} \quad I-(4)$$

with

$$V_i = \bar{Z} \left[ \frac{z}{r} + \int \frac{[\bar{Z} \rho_i(\vec{r}') - \rho_e(\vec{r}')]}{|\vec{r} - \vec{r}'|} d\vec{r}' \right] \quad I(5)$$

These coupled equations are solved self-consistently. In equation I(1)-I(5),  $\rho_e(\vec{r})$  and  $\rho_i(\vec{r})$  are the electron and ion distribution,  $\bar{Z}$  is the mean ionic charge ( $\bar{Z} = Z - n_b$ ) the number of bound electrons.  $R$  is the radius (approximately the ion sphere radius) over which charge neutrality is achieved.  $f$ 's are the occupation factors. For ion of a particular configuration,  $f_b$ 's are integral occupation factors for the bound states of the ion. In contrast; for 'average atom model', the  $f$ 's are taken to be Fermi distribution functions with fractional occupation,  $\phi_b$ 's are the bound and  $\phi_{kl}$ 's are the continuum wavefunctions of energy  $k^2/2$  and angular momentum 1. The exchange-correlation potential is denoted by  $V_{xc}$ . It depends on the plasma density and the temperature and is calculated<sup>2,3</sup> separately by summing up the exchange and "ring" diagram sums and then used as input to subsequent calculations in eq. I(1)-I(5).

Let us point out that the effective ionic charge  $\bar{Z}$  ( $= Z - n_b$ ,  $n_b$  is the number of bound electrons) is an essential ingredient to the calculation. In our model, an 'average atom' model-type calculation is done first to generate  $Z$ . For this; equations I-(1) through I-(5) are solved numerically to self-consistency with  $f_b$ 's and  $f(k)$ 's in eq. I-(3) taken as Fermi functions (i.e. fractional occupation numbers).

Once  $\bar{Z}$  is generated from self-consistent 'average atom' type model as outlined above, it is then used as input to subsequent iterative calculation. Thus, eq. I-(1) through I-(5) are solved numerically to self-consistency with  $f_b$ 's taken to be integral occupation factors corresponding to the ion of specific

configurations, (for example, for Ne-like ground state:  $1S^2 2S^2 2p^6$ ;  $f_b$ 's are 2 for  $1S$ -state; 2 for  $2S$ -state and 6 for  $2p$ -state). This is the important difference between our model for ions of specific configuration and the 'average atom' type model<sup>4</sup>.

Once the self-consistent potentials for ions in plasmas are obtained, the bound-free, bound-bound and free-free cross sections can be computed by generating the relevant numerical bound and continuum wavefunctions first and then computing the relevant matrix elements. These photoprocesses will be outlined in the next section.

## II BOUND-BOUND PHOTOPROCESS

For absorption of a photon of energy  $\hbar\omega$  in a spectrum line so that an electron makes a transition from one ionic state  $\chi_a$  to another  $\chi_b$ :



the photon frequency is close to the line-center frequency  $\omega_0$ :

$$\hbar\omega_0 = E_b - E_a \quad (\text{II-2})$$

The contribution to the monochromatic opacity  $K_\omega$  due to (II-1) is:

$$K_\omega(a \rightarrow b) = \frac{2\pi^2 e^2}{mc} N_a f(b,a) \phi_\omega \quad (\text{II-3})$$

where  $N_a$  is the number density of ions  $X_a$ ,  $\phi_\omega$  is a profile factor normalized to:

$$\int \phi_{\omega} d\omega = 1 \quad (\text{II-4})$$

and  $f(b,a)$  is the oscillator strength given by<sup>9</sup>:

$$f(b,a) = \frac{2m}{e^2 h} \omega_0 \frac{S(b,a)}{3g_a} \quad (\text{II-5})$$

where  $S(b,a)$  is the line strength:

$$S(b,a) = |\langle b || D || a \rangle|^2 \quad (\text{II-6})$$

with the operator  $D$  is dipole operator.

If the bound-state wave functions (numerically generated from the self-consistent potential) are represented as:

$$\Psi_{lm}(\vec{r}) = Y_{lm}(\hat{r}) \frac{P_l(r)}{r} \quad (\text{II-7})$$

where  $Y_{lm}(\hat{r})$  is the spherical harmonic. Then,

$$\begin{aligned} S(l,l') &= \sum_{mm'} |\langle lm | \vec{r} | l'm' \rangle|^2 \\ &= \sum_{mm'q} |\langle lm | r_q^{(1)} | l'm' \rangle|^2 \\ &= l > \left[ \int P_l P_{l'} r dr \right]^2 \end{aligned} \quad (\text{II-8})$$

Where  $l, l'$  are the angular momentum values;  $m, m'$  are the Z components and  $l >$  is the greater of the  $l$  values considered.

### III BOUND-FREE PHOTOPROCESSES (PHOTOIONIZATION)

For photoionization; we replace  $\psi_{l'm'}$  by  $\tilde{\psi}_{l'm'}$  defined by:

$$\tilde{\psi}_{l'm'} = \sqrt{\frac{2}{\pi}} Y_{l'm'}(\hat{r}) \frac{1}{r} F_{k'l'}(r) \quad (\text{III-1})$$

with

$$F_{k'l'}(r) \xrightarrow[r \rightarrow \infty]{} \frac{1}{\sqrt{k'}} \sin(k'r + \dots) \quad (\text{III-2})$$

for normalization condition for  $\tilde{\psi}_{l'm'}$  is:

$$\int \langle \tilde{\psi}_{lmE} | \tilde{\psi}_{lmE'} \rangle dE' = 1 \quad (\text{III-3})$$

and

$$\langle \tilde{\psi}_{lmE} | \tilde{\psi}_{lmE'} \rangle = \delta(E - E')$$

The oscillator strength for photoionization is given by:

$$\frac{df}{dE} = \frac{4}{3\pi} \frac{\omega}{(2l+1)} \sum_{l'} \left[ \int p_{l'} F_{k'l'} r dr \right]^2 \quad (\text{III-4})$$

### IV FREE-FREE TRANSITIONS

To obtain the oscillator strength  $df/dE$  for photoabsorption of one photon  $\omega$  in the field of an ion in a plasma of electron density  $N_e$  of mono-

energetic electrons, we replace  $\psi_{l'm'}$  in the expression for bound-bound by  $\tilde{\psi}_{l'm'}$  and  $\psi_{lm}$  by  $\tilde{\psi}_{lmk}$  which represents the lm component of the total function describing the flux of electrons having momentum  $\vec{k}$ . For isotropic distribution of velocities, such function has the asymptotic form

$$\Psi \rightarrow \sqrt{\frac{1}{4\pi} N_e} e^{i \vec{k} \cdot \vec{r}} \quad (\text{if } rV \rightarrow 0) \quad (\text{IV-1})$$

(and an analogical expression for Coulomb Field).

It can be shown that, the oscillator strength for the free-free process is given by:  
(see Appendix I for a proof)

$$\frac{df}{dE} = \frac{16}{3} N_e \frac{1}{k\omega^3} \sum_{ll'} | \int F_{kl} F_{k'l'} \frac{dv}{dr} dr |^2 \quad (\text{IV-2})$$

## V MODEL FOR DISTRIBUTION OF IONIC SPECIES IN PLASMAS

For calculation of overall radiation absorption and opacities, it is necessary to know the distribution (i.e. number densities) of ions of different types that occur in plasma at a particular density and temperature. It is possible to obtain these distributions from detailed rate equation calculations. The computation involved in rate equation solution is time-consuming, complex and tedious. Here we discuss an alternative approach. This model is based on the density functional method, following Perrot.<sup>8</sup> This is outlined below to point out specific aspects of the calculation involved.

Opacities of plasmas have often been calculated using 'average atom' model (AAM) for ionic species. The AAM, however, deals with fictitious 'average atom' with fractional occupation of electronic bound states. In a real plasma, a number of different ionic species are usually present in various abundance.

Let us first consider the total energy of an ionic species defined by the configuration of the bound spectrum and a screening charge of free electrons in LTE. The fixed integer occupation numbers of bound electrons are  $n_i$ 's while the fractional occupation numbers of free electrons are denoted by  $f_k$ 's. The total energy considered here is that of embedding the atom in the plasma:

$$\Delta E (\dots n_i \dots) = E (\dots n_i, \dots) - \bar{E} [\bar{\rho}] \quad (V-I)$$

where  $\bar{E} (\bar{\rho})$  is the unperturbed electron gas energy. One can show that<sup>8</sup>

$$\begin{aligned} \Delta E (\dots n_i, \dots) &= \sum_i n_i \epsilon_i + \frac{2}{\pi} \sum_L (2L+1) \int_0^{\infty} f_k \frac{dn_L}{dk} \frac{k^2}{2} dk \\ &+ \langle \bar{\rho} 2\pi r^2 (\rho_b + \rho_i - \bar{\rho}) \rangle - \frac{1}{2} \langle (\rho_b + \rho_i - \bar{\rho}) \frac{1}{r} \circ (\rho_b + \rho_i - \bar{\rho}) \rangle \\ &+ E_{xc}^o (\rho_b) - \langle \rho_b [V_{xc}^o (\rho_b) + W_{xc} (\rho_b, \bar{\rho})] \rangle + \end{aligned}$$

$$E_{xc}^T(\rho_i) - E_{xc}^T(\bar{\rho}) - \langle \rho_i v_{xc}^T(\rho_i) \rangle - \langle (\rho_b + \rho_i) v_{xc}^T(\bar{\rho}) \rangle \\ - \frac{3}{2} \frac{Z_c}{R_c} [Z - \frac{3}{5} Z_c] \quad (V-2)$$

In (V-2); the notations

$$\langle fg \rangle = \int f(\vec{r}) g(\vec{r}) d\vec{r} \\ f \circ g = \int f(\vec{r}') g(\vec{r} - \vec{r}') d\vec{r}'$$

and

(convolution product)

have been used.

In (V-2),  $\rho_b$  is the bound and  $\rho_i$  the free electron density,  $\eta_L$  the phase of the continuum electronic states,  $\bar{\rho}$  the mean electron density of the plasma;  $E_{xc}^T$  is the exchange-correlation energy, and  $W_{xcb}$  is the bound-free exchange-correlation potential.

Next, consider the transition of an electron from initial state  $i$  to final state  $j$  in the bound spectrum. The change in the total energy of the species associated with the transition is:

$$\delta E_{Z^*}(i \rightarrow j) = \Delta E(-\dots n_i=0, \dots n_j=1, \dots) \\ - \Delta E(-\dots n_i=1, \dots n_j=0, \dots) \quad (V-3)$$

In above,  $Z^*$  refers to the ionization degree of the species. Energies in eq. (V-3) are defined by eq. (V-1). The 'transition-state' theory of Slater is utilized in the calculation here. It improves on the AAM which has been used often to obtain the average degree of ionization in a plasma.

In a plasma of different ionic species, let us consider the most abundant species with a given ionization degree  $Z^*$ . The energy of this one, which has the configuration  $\langle \dots n_{i_0} \dots \rangle$  is chosen as a reference. The total energy of another species with the same  $Z^*$  but a different configuration  $\{\dots n_i \dots\}$  can be shown to

be:

$$\Delta E_{Z^*} (-\dots n_{i_0}) + \sum \epsilon_{iz^*}^* \Delta n_i + O(\Delta n^2) \quad (V-4)$$

where  $\sum \epsilon_{iz^*}$  is the modified effective energies of the referenced species, provided that

$$\sum \Delta n_i = \sum (n_i - n_{i_0}) = 0 \quad (V-5)$$

bound bound

The system can now be interpreted as a collection of independent pseudoparticles, distributed among states of energy  $\epsilon_{iz^*}$ . The average occupation numbers for the species will be given by FD statistics,

$$\bar{n}_i = 1 / \{ 1 + \exp [ \beta (\epsilon_{iz^*} - \mu_{z^*}) ] \} \quad (V-6)$$

$\mu_{z^*}$  is our effective chemical potential for the bound pseudoparticles, to be determined from

$$\sum \bar{n}_i = Z - z^* . \quad (V-7)$$

Equations (V-6) and (V-7) thus fully define the average species for the ionization degree  $Z^*$ . Finally, the probability of a  $Z^*$  species is given by

$$P_{z^*} = A \exp (-\beta F_{z^*}) \quad (V-8)$$

where  $F_{z^*}$  is the effective free energy which can be obtained from the  $\Delta E_{Z^*}$

(... $\bar{n}_i$ , ...) discussed above and the entropy of the bound pseudo-particles.

$$S_{Z^*} = -k_B \sum [\bar{n}_i \ln \bar{n}_i + (1-\bar{n}_i) \ln (1-\bar{n}_i)] \quad (V-9)$$

In (V-8), A is a normalization constant such that  $\sum p_{Z^*} = 1$ , the sum running over all integer ionization states,

and

$$F_{Z^*} = \Delta E_{Z^*} (\dots, \bar{n}_i, \dots) - TS_{Z^*} - T\Delta S [p_i] \quad (V-10)$$

is the effective free-energy determining the probability via eq. (V-8).

As an example of the application of this model<sup>8</sup>, consider probabilities of various ionic species in the Aluminum plasma at temperature 100 eV and electron density of  $4.8 \times 10^{23} \text{ cm}^{-3}$ . The average atom model gives the average ionization degree for the plasma in the above condition as 7.9. This indicates that the effective ion charge  $Z^* = 8$  (i.e. ions with 5 bound electrons or Boron-like ions) will have the highest probability of occurrence. This is confirmed from the calculation using the above model<sup>8</sup>:  $P_{Z^*}$  is highest for  $Z^* = 8$  and drops off rapidly for lower and higher  $Z^*$  ionic species. The relative abundances of ions of different species in the Al-plasma at the above density and temperature are thus obtained.

It is seen<sup>8</sup> that for the above plasma conditions B-like Al is most abundant, followed by Be-like, C-like, O-like, Li-like ions etc. in decreasing order of relative abundances. Thus the model discussed above provides an useful tool to generate the number densities (or abundances) of different ionic species in a plasma. These data are necessary for subsequent computation of radiation absorption in a plasma.

Note that the distribution of ionic species in plasmas are usually obtained by solution of rate equations. The rate equation method, however, is

very complex, tedious and time-consuming. In view of the advantages of the model discussed above, we are in the process of building a computer code in order to generate the ionic distribution in different plasma conditions.

## VI ELECTRICAL CONDUCTIVITY IN HOT DENSE PLASMAS

Electron conduction is important in absorption of radiation from lasers because low frequency inverse bremsstrahlung is essentially the same as Ac joule heating. Emission of visible and ultraviolet light (and generation of magnetic field) also involve electron current flow. Electron heat conduction is an important limitation on thermonuclear burn and is particularly important in laser-target ablation. The energy transported by electron conduction, in turn, determines conductive opacity.

In this section, we discuss a model to compute electrical conductivity (or resistivity) of dense plasmas. Various methods, such as Kubo approach or Boltzmann transport eqn. method has been used by different groups to obtain electrical conductivity<sup>7</sup> (or resistivity) in plasmas. A successful approach is via Ziman formula<sup>6</sup> which is essentially a variational solution to Boltzmann eqn. Following Perrot and Dharma-Wardana<sup>5</sup>, the method we will discuss here is a generalization of Ziman formula using density functional method. This extends the applicability from the usual weak-isolated-scatterer limit to the regime of strong multiple scatterers, as is important for high density plasmas.

### a) REGIME OF ISOLATED SCATTERERS

The most familiar form of Ziman formula applies to plasmas and liquid metals in regime of weak and strong but isolated scatterers. The resistivity  $R$  is given by,

$$R = \frac{\hbar}{3\pi\bar{Z}^2e^2\rho} \int_0^\infty d\epsilon f'(\epsilon) \int_0^{2k} dq q^3 S(q) \sigma(q) \quad (\text{VI-1})$$

where  $q^2 = 2k^2(1 - \cos\theta)$ . Here  $q$  is the momentum transferred from the incident electron with energy  $\epsilon = k^2$ . The derivative of the Fermi distribution function for electrons at a mean density  $\bar{n} = \bar{Z}\bar{\rho}$  is denoted by  $f'(\epsilon)$ . The mean

ion density is  $\bar{\rho}$ . The ion distribution is specified by the structure factor  $S(q)$ . The differential scattering cross-section  $\sigma(q)$  depends on the incident electron momentum  $\vec{k}$  and the transferred momentum  $\vec{q}$ . For strong scatterers  $\sigma(q)$  has to be obtained from the phase shifts of  $V_{ei}$ .

In the weak isolated scatterer limit, the Born approximation may be used to obtain  $\sigma(q)$ :

$$\sigma(q) = |V_{ei}(q) / 4\pi \epsilon(q)|^2 \quad (\text{VI-2})$$

In above  $V_{ei}(q)$  is the weak electron-ion interaction, and  $\epsilon(q)$  is the exact interacting uniform electron-gas dielectric function at a density  $\bar{n}$  and temperature  $T$ . The density functional method outlined previously is capable of generating  $\epsilon(q, n, T)$  also.

The ion-ion structure factor  $S(q)$  (VI-1) is determined by the ion density  $\bar{\rho}$ , temperature  $T$ , and the ion-ion pair interaction  $V_{ii}(q)$ . In the DFM model of calculation for single ions immersed in an electron gas, the Kohn-Sham equations are solved numerically for continuum electron states  $\phi_{kl}(r)$  which incorporates the appropriate phase shifts  $\delta_l(k)$ . At self-consistency, the phase shifts satisfy the finite temperature version of the Friedel sum rule, thus assuring the correct construction of the continuum electron density of states as modified by the scattering potential. The scattering cross-section is given in terms of the phase shifts by:

$$\begin{aligned} \sigma(q, \theta) &= t_{kk'}(\epsilon) \\ &= \left| \frac{1}{2ik} \sum_l (2l+1) \left( e^{2i\delta_l(k)} - 1 \right) P_l(\cos \theta_{kk'}) \right|^2 \end{aligned} \quad (\text{VI-3})$$

The scattering angle  $\theta$  and the momentum transferred

$\vec{q} = \vec{k}' - \vec{k}$  is related by

$$q^2 = 2k^2 (1 - \cos \theta) \quad (\text{VI-4})$$

For elastic scattering  $k^2 = k'^2 = \epsilon$ .

### b) THE REGIME OF STRONG MULTIPLE SCATTERERS

The ion-ion interactions in this regime cannot be treated as a sum of independent scattering centers, either for weak or strong scatterers. Thus, the electron is scattered from a given quasi-static ion distribution consisting of many centers. For a definite configuration C of ions, the resistivity can be written as :

$$R_e = \frac{t}{3\pi e^2 n^2} \int_0^\infty d\epsilon \tilde{f}'(\epsilon) \int_0^{2K} dq q^3 T_{kk'}^C(\epsilon) \quad (\text{VI-5})$$

In the DFM method, the T-matrix for the given a configuration C is approximated by  $\bar{T}_{kk'}$ , where  $\bar{T}_{kk'}(\epsilon)$  is calculated from the average-ion distribution  $\rho(r)$ . The total T-matrix of the average distribution  $\bar{T}_{kk'}(\epsilon)$  is obtained from the phase shifts  $\Delta_l(k)$  of the Kohn-Sham equation solved in the external field of the scattering ion and its associated distribution  $\rho(r)$ . In the isolated scatterer limit,

$$T_{kk'}(\epsilon) \rightarrow \bar{\rho} S(|\vec{k}-\vec{k}'|) t(|\vec{k}-\vec{k}'|) \quad (\text{VI-6})$$

In general, the modified fermi function  $\tilde{f}$  in eqn. (VI-5) needs to be calculated from one-particle Green's function with self-energy correction.

Perrot et al<sup>5</sup> have shown that eqn. (VI-5) can be simplified to

$$R = \frac{\hbar}{3\pi^2 e^2 n^2} \int_0^\infty d\varepsilon f'(\varepsilon) \int_0^{2k} dq q^3 \bar{T}(q) \quad (\text{VI-7})$$

for strong multiple scatterers.

It is clear from above discussion of the model that the structure factor  $S(\vec{k})$  and the T-matrix of the average-ion distribution  $\bar{T}_{kk'}(\varepsilon)$  are crucial ingredients in the calculation of resistivity of dense plasmas inclusive of strong multiple scattering effect. In our self-consistent calculation, we can generate the structure factor by taking fourier transform of pair correlation function which, in turn, is generated from charge distributions obtained self-consistently. The phase shifts  $\Delta_l(k)$  in the field of the scattering ion and its associated distribution  $\rho(r)$  can also be generated by our atomic codes. We are, therefore, in a position to utilize the model discussed above to calculate electron conductivity inclusive of multiple scattering effects. Let us note that the energy transported by electron conduction, in turn, determines conductive opacity. However, conductive opacity dominates over radiative opacity only at super high densities (i.e. for extremely degenerate plasmas). For most laboratory plasmas, conductive opacity is small compared to radiative opacity.

## RESULTS

The calculations for the atomic processes contributing to absorption of radiation involve development of several computer codes. A large part of the work for the project involved development, modification, testing and benchmarking a set of computer codes for different plasma conditions.

For the project, the following set of codes were either set up or modified according to the models discussed in the preceding sections:

1. An 'average atom' code for dense plasmas according to the prescription of finite temperature density functional method<sup>11</sup> (This is very similar to the model used by Liberman<sup>10</sup>).
2. An atomic structure code for isolated multielectron ions of specific configurations.
3. A self-consistent atomic structure code for multielectron ions of specific configuration immersed in a plasma. This includes plasma screening and other effects discussed in Section I.
4. A code to compute bound-free photoionization cross-sections for isolated ions. (Also a relativistic photoionization code applicable for high Z-elements).
5. A code to compute photoionization cross-sections of ions of specific configuration inclusive of dense plasma effects.
6. A self-consistent code to generate free-free photoprocesses for ions of given configuration inclusive of plasma effects. Full numerical continuum wavefunctions in self-consistent potentials are used in calculating matrix elements for free-free transitions in this code.
7. A code to compute bound-bound photo-excitation cross-sections for ions of specific configurations inclusive of plasma effects.

For a given plasma condition (i.e. at a given density  $n_e$  and temperature  $T$ , first a self-consistent calculation using 'average atom' code is done to obtain the effective or 'average' ionic charge  $\bar{Z}$ . This is then used in subsequent calculations. For an ion of specific configuration immersed in the plasma of the above density  $n_e$  and temperature  $T$ , the self-consistent code described in Sec. I is used to generate energy levels, wavefunctions, self-consistent ionic

potentials and other quantities. Then calculations for bound-bound photoexcitation, bound-free photoionization and free-free photoprocesses are done utilizing the numerical wavefunctions etc. The free-free cross-sections for an ion are calculated for various angular momentum states ( $l$ -values) for a given photon energy. The allowed transitions are, of course, between continuum states of angular momentum  $l$  and  $|l \pm 1|$ . All the contributions from different  $l$  values are summed up to obtain the resultant oscillator strength of  $df/dE$ .

For purpose of illustration, we now discuss some representative results. Results are tabulated for self-consistent calculations of aluminum plasma at electronic density  $n_e = 2.2 \times 10^{23} \text{ cm}^{-3}$  and temperature  $T = 50 \text{ eV}$ . Computed data for bound-free oscillator strengths (Ryd $^{-1}$ ) for photon energies in the range 0.01 - 100 Ryd. are tabulated in Tables 1-3 for Ne-like ion ( $1S^2 2S^2 2p^6$ ) in the plasma in above condition. Table 1 is for photoionization from  $1S$ -state, Table 2 for  $2S$ -state and Table 3 for  $2p$ -state. The typical variation of bound-free oscillator strength is seen to be a rapid rise from threshold, going through a peak, then a sharp decrease followed by a gradual decrease with increasing photon energy. This is seen clearly from Fig. 1. Results for other types of ions:  $1S^2 2S^2 2p^5$  (Tables 4-6);  $1S^2 2S^2 2p^4$  (Tables 7-9);  $1S^2 2S^2 2p^6 3S$  (Tables 10-12) in Aluminum plasma at electron density  $n_e = 2.2 \times 10^{23} \text{ cm}^{-3}$  and  $T = 50 \text{ eV}$  over the range of photon energy 0.01 - 100 eV are also tabulated.

The oscillator strengths for free-free photoprocesses for Ne-like Al in an Aluminum plasma  $n_e = 2.2 \times 10^{23} \text{ cm}^{-3}$ ,  $T = 50 \text{ eV}$  for a set of photon energies are given in Tables 13-20. Full numerical continuum wavefunctions in self-consistent potentials are used in evaluating the allowed  $l \rightarrow |l \pm 1|$  transitions and eqn. (IV-2) is used in calculating the matrix elements for oscillator strengths for a range of incident electron energies. This method of calculating free-free cross-sections clearly is an improvement over semi-classical approximations such as Born-Elwert method<sup>12</sup>. For purpose of comparison, results of free free calculations using unscreened Coulomb potential for Ne-like Al (instead of self-consistent screened potential) are also given. The computer

output for free-free cross sections display the relevant matrix elements for different  $l$  values. For each photon energy, oscillator strengths are shown in the computer printout for a set of incident electron energies  $E_{in}$ 's. The  $E_{in}$ 's considered are 1.0, 2.0, 5.0, 10.0, 20.0, 30.0, 50.0 at units. The large difference in oscillator strengths for the same photon energies for self-consistent results with those of unscreened Coulomb potential show the importance of including plasma effects appropriately in the calculations.

As an example of a typical bound-free calculation, a sample computer output of photoionization from 1S-state of Ne-like Al in Al plasma is attached. The self-consistent potential is supplied as input. The output shows some of the radial mesh points and the corresponding potential, the iterative process (by Numerov method) of solving the energy eigenvalue of the 1S-state. For each photon energy, the corresponding bound-free matrix element and the cross-section is computed and tabulated. The data corresponds to those of Table 1.

As an example of the codes used for the calculations, the listing of FFNEW.FOR for generating free-free oscillator strengths for  $l \rightarrow (l+1)$  transitions is also attached. Again, self-consistent potential for an ion in a plasma is fed in as input read by subroutine VREAD. OMEGA is a typical photon energy in atomic units, FFOSC is the oscillator strength summed over all continuum states. Numerical derivative of the potential is used in the calculation of matrix elements. The associated subroutines DIFF.FOR and SIMP.FOR are also attached. DIFF generates the numerical continuum wavefunctions. Minor changes are needed in FFNEW.FOR for calculating  $l \rightarrow (l-1)$  transitions for different photon energy OMEGA. The incident electron energy EIN is read in; EOUT is the outgoing electron energy ( $EOUT = EIN + OMEGA$ ).

For overall calculations of opacities, other effects such as line broadening and scattering of photons need to be properly included in the calculation. We are in the process of building up the necessary computer codes to combine these effects in the overall computation of radiative opacity of dense plasmas.

## CONCLUSIONS

A number of self-consistent models and computer codes have been developed which are very useful for investigating the large number of atomic processes contributing to radiation absorption in dense plasmas. The important effects arising in dense plasmas -- non linear screening, electron exchange-correlation and degeneracy, strong ion coupling etc. are systematically included in these models. These are applicable to ions of specific configurations in dense plasmas and thus represent improvements over average atom models. These methods are particularly useful in moderately high densities ( $\sim 10^{23} - 10^{24}$  e/cm<sup>3</sup>) and relatively lower temperature range ( $\sim 10$  eV-200 eV) where average atom models are known to be inadequate.

A large number of atomic processes contribute to radiation absorption in plasmas. Most of the work for this project dealt with bound-bound, bound-free and free-free photoprocesses for ions in dense plasmas. The self-consistent calculations are involved and time-consuming (particularly since the VAX-8350 is the only computer we could use for this project and we did not have access to Cray, for example). For overall calculation of opacities in wide range of plasma conditions, vast atomic data bases need to be generated involving enormous amounts of computation. We hope to address those tasks in future years.

---

This work was supported by the Air Force Office of Scientific Research

## ACKNOWLEDGEMENTS

The author wishes express sincere thanks to Dr. Robert J. Barker, AFOSR, for sponsoring this work, and to thank Dr. Milan Blaha of the University of Maryland for useful discussions and his assistance in computational work. Thanks are also due to Mrs. Karla Walker of SFA for VAX-8350 systems support, and Mrs. Renee Knoch of SFA for putting this Final Report together.

## REFERENCES

1. See, for example, J.P. Cox and R.T. Giuli, "Principles of Stellar Structure" (Gordon and Breach Science Publishers, New York) (1984).
2. U. Gupta and A.K. Rajagopal, Phys. Rev. A 22, 2792 (1980).
3. F. Perrot and M.W.C. Dharma-Wardana, Phys. Rev. A 30, 2619 (1984).
4. For a review, see, for example, R. More in "Atomic Physics In Inertial Confinement Fusion," Univ. of California Report No. UCRL-88511 (1982).
5. F. Perrot and M.W.C. Dharma-Wardana, Phys. Rev. A 36, 238 (1987).
6. J.M. Ziman, Philos. Mag. 6, 1013 (1961).
7. George A. Rinker, Phys. Rev. B 31, 4207 (1985).
8. F. Perrot, Phys. Rev. A 35, 1235 (1987).
9. M.J. Seaton, J. Phys., B. 20, 6363 (1987).
10. D.A. Liberman, Phys. Rev. B 20, 4981 (1979).
11. U. Gupta and A.K. Rajagopal, Review Article in Physics Reports 87, No. 6 (North Holland Publishing Co., 1982).
12. I.P. Grant, Proceedings of Royal Society, No.3, 118, 241 (1958).
13. R.P. Feynman, N. Metropolis and E. Teller, Phys. Rev. 75, 1561 (1949)
14. R.S. Cowan and J. Ashkin, Phys. Rev. 150, 144 (1957).

## APPENDIX I

### FREE-FREE TRANSITIONS

For deriving eqn. (IV-2) we write the wave function as:

$$\begin{aligned}\bar{\Psi} &= \sqrt{\frac{N_e}{4\pi}} \sum_l (2l+1) i^l P_l(\hat{k} \cdot \hat{r}) K^{-1/2} \frac{F_{kl}}{r} \\ &= \sqrt{\frac{N_e}{4\pi}} \sum_l (2l+1) i^l \frac{4\pi}{(2l+1)} \sum_m Y_{lm}^*(\hat{k}) Y_{lm}(\hat{r}) K^{-1/2} \frac{F_{kl}}{r}\end{aligned}$$

Therefore

$$\bar{\Psi}_{lmk} = \sqrt{4\pi N_e} i^l Y_{lm}^*(\hat{k}) Y_{lm}(\hat{r}) K^{-1/2} \frac{F_{kl}}{r}$$

Total oscillator strength per ion is equal to the sum of all possible contributions:

$$\frac{df}{dE} = \frac{2}{3} \omega \sum_{ll'mm'} \int | \langle \bar{\Psi}_{lmk} | \vec{r} | \bar{\Psi}_{l'm'k'} \rangle |^2 d\hat{k}$$

$\tilde{\psi}_{l'm'k'}$  does not depend on direction  $\hat{k}'$  of the scattered electron, the averaging over angles gives just the form of  $\tilde{\psi}$  used here,  $\omega$  is the photon frequency.

Since

$$\int Y_{lm}^*(\hat{k}) Y_{lm}(\hat{k}) d\hat{k} = 1$$

$$\begin{aligned}\frac{df}{dE} &= \frac{2}{3} \omega \sum_{ll'mm'} 4\pi N_e \bar{k}^1 \frac{2}{\pi} |\langle lm | \vec{r} | l'm' \rangle|^2 \\ &\quad * \left[ \int F_{kl} r F_{k'l'} dr \right]^2 \\ &= \frac{16}{3} N_e \bar{k}^1 \omega \sum_{ll'} l' \left[ \int F_{kl} r F_{k'l'} dr \right]^2\end{aligned}$$

Since

$$\left| \int F_{kl} F_{k'l'} r dr \right| = \frac{1}{\omega^4} \left| \int F_{kl} F_{k'l'} \frac{dv}{dr} dr \right|$$

we have

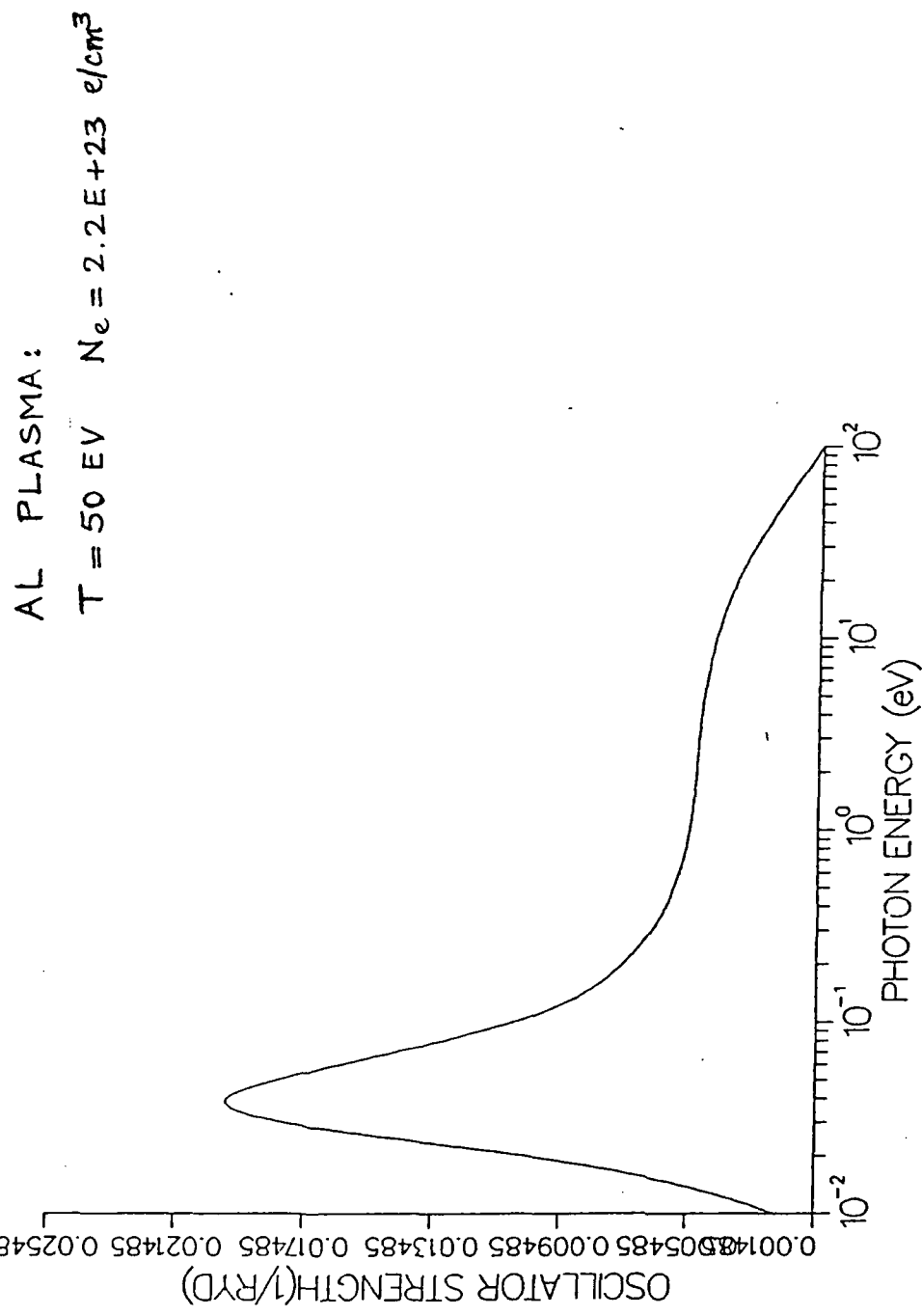
$$\frac{df}{dE} = \frac{16}{3} N_e k^{-1} \omega^{-3} \sum_{ll'} l_l l_{l'} \left| \int F_{kl} F_{k'l'} \frac{dv}{dr} dr \right|^2.$$

This proves eqn. (IV-2).

**FIGURE 1**

FIGURE 1

NE LIKE AL - PHOTOIONIZATION FROM 1S - LEVEL



## **TABLES**

TABLE 1

OSCILLATOR STRENGTH FOR PHOTOIONIZATION FROM 1S-LEVEL

NE-LIKE AL:  $1s^2 2s^2 2p^6$ 

ELECTRON DENSITY=2.2E+23 TEMP=50 EV

PHOTON ENERGY(RYD)	OSC. STRENGTH(1/RYD)
0.01	0.2729E-02
0.02	0.1053E-01
0.03	0.1829E-01
0.04	0.1983E-01
0.05	0.1810E-01
0.10	0.1084E-01
0.20	0.7484E-02
0.50	0.5958E-02
1.00	0.5477E-02
2.00	0.5295E-02
5.00	0.5059E-02
10.00	0.4698E-02
12.00	0.4563E-02
15.00	0.4371E-02
20.00	0.4069E-02
30.00	0.3530E-02
50.00	0.2682E-02
100.00	0.1485E-02

TABLE 2

OSCILLATOR STRENGTH FOR PHOTOIONIZATION FROM 2S-LEVEL

NE-LIKE AL:  $1s^2 2s^2 2p^6$ 

ELECTRON DENSITY=2.2E+23 TEMP=50 EV

PHOTON ENERGY(RYD)	OSC. STRENGTH(1/RYD)
0.01	0.9451E-02
0.02	0.3644E-01
0.03	0.6331E-01
0.04	0.6857E-01
0.05	0.6257E-01
0.10	0.3740E-01
0.20	0.2569E-01
0.50	0.2018E-01
1.00	0.1814E-01
2.00	0.1679E-01
5.00	0.1419E-01
10.00	0.1098E-01
12.00	0.9983E-02
15.00	0.8713E-02
20.00	0.7046E-02
30.00	0.4814E-02
50.00	0.2552E-02
100.00	0.8175E-03

TABLE 3

OSCILLATOR STRENGTH FOR PHOTOIONIZATION FROM 2P-LEVEL

NE-LIKE AL:  $1S^2 2S^2 2P^6$ 

ELECTRON DENSITY=2.2E+23 TEMP=50 EV

PHOTON ENERGY(RYD)	OSC. STRENGTH(1/RYD)
0.01	0.1027E-02
0.02	0.1101E-02
0.03	0.1185E-02
0.04	0.1366E-02
0.05	0.1683E-02
0.10	0.6747E-02
0.20	0.3191E-01
0.50	0.2787E-01
1.00	0.2268E-01
2.00	0.2009E-01
5.00	0.1563E-01
10.00	0.1068E-01
12.00	0.9262E-02
15.00	0.7537E-02
20.00	0.5464E-02
30.00	0.3092E-02
50.00	0.1237E-02
100.00	0.2478E-03

TABLE 4

OSCILLATOR STRENGTH FOR PHOTOIONIZATION FROM 1S-LEVEL

AL ION :  $1s^2 2s^2 2p^5$ 

ELECTRON DENSITY=2.2E+23 TEMP=50 EV

PHOTON ENERGY(RYD)	OSC. STRENGTH(1/RYD)
0.01	0.1006E-02
0.02	0.3188E-01
0.03	0.5733E-02
0.04	0.7858E-02
0.05	0.9296E-02
0.10	0.1008E-01
0.20	0.7977E-02
0.50	0.6076E-02
1.00	0.5545E-02
2.00	0.5315E-02
5.00	0.5069E-02
10.00	0.4704E-02
12.00	0.4569E-02
15.00	0.4376E-02
20.00	0.4075E-02
30.00	0.3538E-02
50.00	0.2689E-02
100.00	0.1487E-02

TABLE 5

OSCILLATOR STRENGTH FOR PHOTOIONIZATION FROM 2S-LEVEL  
 AL ION :  $1s^2 2s^2 2p^5$   
 ELECTRON DENSITY=2.2E+23 TEMP=50 EV

PHOTON ENERGY( RYD )	OSC. STRENGTH( 1/RYD )
0.01	0.3482E-02
0.02	0.1103E-01
0.03	0.1982E-01
0.04	0.2716E-01
0.05	0.3211E-01
0.10	0.3473E-01
0.20	0.2737E-01
0.50	0.2056E-01
1.00	0.1835E-01
2.00	0.1684E-01
5.00	0.1420E-01
10.00	0.1098E-01
12.00	0.9976E-02
15.00	0.8704E-02
20.00	0.7038E-02
30.00	0.4809E-02
50.00	0.2550E-02
100.00	0.8165E-03

TABLE 6

OSCILLATOR STRENGTH FOR PHOTOIONIZATION FROM 2P-LEVEL

AL ION :  $1s^2 2s^2 2p^5$ 

ELECTRON DENSITY=2.2E+23 TEMP=50 EV

PHOTON ENERGY(RYD)	OSC. STRENGTH(1/RYD)
0.01	0.1787E-02
0.02	0.1538E-02
0.03	0.1462E-02
0.04	0.1504E-02
0.05	0.1652E-02
0.10	0.4203E-02
0.20	0.1878E-01
0.50	0.2823E-01
1.00	0.2303E-01
2.00	0.2015E-01
5.00	0.1564E-01
10.00	0.1070E-01
12.00	0.9277E-02
15.00	0.7551E-02
20.00	0.5476E-02
30.00	0.3097E-02
50.00	0.1237E-02
100.00	0.2477E-03

TABLE 7

OSCILLATOR STRENGTH FOR PHOTOIONIZATION FROM 1S-LEVEL

AL ION:  $1s^2 2s^2 2p^4$ 

ELECTRON DENSITY=2.2E+23 TEMP=50 EV

PHOTON ENERGY(RYD)	OSC. STRENGTH(1/RYD)
0.02	0.7035E-02
0.03	0.7789E-02
0.04	0.8168E-02
0.05	0.8333E-02
0.10	0.8253E-02
0.20	0.7312E-02
0.50	0.5549E-02
1.00	0.5595E-02
2.00	0.5368E-02
5.00	0.5075E-02
10.00	0.4704E-02
12.00	0.4569E-02
15.00	0.4376E-02
20.00	0.4075E-02
30.00	0.3540E-02
50.00	0.2694E-02
100.00	0.1488E-02

TABLE 8

OSCILLATOR STRENGTH FOR PHOTOIONIZATION FROM 2S-LEVEL

AL ION:  $1s^2 2s^2 2p^4$ 

ELECTRON DENSITY=2.2E+23 TEMP=50 EV

PHOTON ENERGY(RYD)	OSC. STRENGTH(1/RYD)
0.02	0.2409E-01
0.03	0.2665E-01
0.04	0.2794E-01
0.05	0.2849E-01
0.10	0.2815E-01
0.20	0.2483E-01
0.50	0.1858E-01
1.00	0.1833E-01
2.00	0.1683E-01
5.00	0.1407E-01
10.00	0.1086E-01
12.00	0.9877E-02
15.00	0.8617E-02
20.00	0.6967E-02
30.00	0.4767E-02
50.00	0.2531E-02
100.00	0.8114E-03

TABLE 9

OSCILLATOR STRENGTH FOR PHOTOIONIZATION FROM 2P-LEVEL

AL ION:  $1s^2 2s^2 2p^4$ 

ELECTRON DENSITY=2.2E+23 TEMP=50 EV

PHOTON ENERGY(RYD)	OSC. STRENGTH(1/RYD)
0.01	0.6903E-03
0.02	0.1471E-02
0.03	0.3150E-02
0.04	0.5769E-02
0.05	0.8491E-02
0.10	0.1799E-01
0.20	0.2966E-01
0.50	0.2515E-01
1.00	0.2264E-01
2.00	0.2001E-01
5.00	0.1544E-01
10.00	0.1057E-01
12.00	0.9169E-02
15.00	0.7469E-02
20.00	0.5422E-02
30.00	0.3069E-02
50.00	0.1225E-02
100.00	0.2461E-03

TABLE 10

OSCILLATOR STRENGTH FOR PHOTOIONIZATION FROM 1S-LEVEL  
 AL ION :  $1s^2 2s^2 2p^6 3s$

ELECTRON DENSITY=2.2E+23 TEMP=50 EV

PHOTON ENERGY(RYD)	OSC. STRENGTH(1/RYD)
0.01	0.5854E-02
0.02	0.6898E-02
0.03	0.7021E-02
0.04	0.6924E-02
0.05	0.6786E-02
0.10	0.6211E-02
0.20	0.5818E-02
0.50	0.5641E-02
1.00	0.5402E-01
2.00	0.5278E-01
5.00	0.5050E-01
10.00	0.4688E-01
12.00	0.4551E-02
15.00	0.4355E-02
20.00	0.4049E-02
30.00	0.3505E-02
50.00	0.2666E-02
100.00	0.1478E-02

TABLE 11

OSCILLATOR STRENGTH FOR PHOTOIONIZATION FROM 2S-LEVEL  
AL ION :  $1s^2 2s^1 2p^6 3s$

ELECTRON DENSITY=2.2E+23 TEMP=50 EV

PHOTON ENERGY(RYD)	OSC. STRENGTH(1/RYD)
0.01	0.2009E-01
0.02	0.2366E-01
0.03	0.2407E-01
0.04	0.2373E-01
0.05	0.2325E-01
0.10	0.2123E-01
0.20	0.1979E-01
0.50	0.1894E-01
1.00	0.1774E-01
2.00	0.1660E-01
5.00	0.1407E-01
10.00	0.1091E-01
12.00	0.9921E-02
15.00	0.8659E-02
20.00	0.7003E-02
30.00	0.4785E-02
50.00	0.2149E-02
100.00	0.8159E-03

TABLE 12

OSCILLATOR STRENGTH FOR PHOTOIONIZATION FROM 2P-LEVEL

AL ION:  $1s^2 2s^2 2p^6 3s$ 

ELECTRON DENSITY=2.2E+23 TEMP=50 EV

PHOTON ENERGY(RYD)	OSC. STRENGTH(1/RYD)
0.01	0.2995E-03
0.02	0.6383E-03
0.03	0.1251E-02
0.04	0.2479E-02
0.05	0.4795E-02
0.10	0.6495E-01
0.20	0.4336E-01
0.50	0.2520E-01
1.00	0.2204E-01
2.00	0.1988E-01
5.00	0.1543E-01
10.00	0.1051E-01
12.00	0.9106E-02
15.00	0.7410E-02
20.00	0.5381E-02
30.00	0.3060E-02
50.00	0.1229E-02
100.00	0.2468E-03

TABLE 13

OSCILLATOR STRENGTH FOR FREE-FREE TRANSITIONS

NEON-LIKE ALUMINUM

ELECTRON DENSITY=2.2E+23 TEMP=50 EV

PHOTON ENERGY=0.370 AT.UNIT

E(INCIDENT) (AT.UNIT)	E(OUTGOING) (AT.UNIT)	OSCILLATOR STRENGTH * (AT.UNIT)
1.00	1.370	0.1980E+01
2.00	2.370	0.8505E+02
5.00	5.370	0.2601E+02
10.00	10.370	0.5506E+02
15.00	15.370	0.9203E+02
20.00	20.370	0.1351E+03
25.00	25.370	0.1830E+03
30.00	30.370	0.2352E+03
50.00	50.370	0.2991E+03
70.00	70.370	0.3707E+03
100.00	100.370	0.4499E+03
150.00	150.370	0.5368E+03
200.00	200.370	0.6281E+03

\* Sum of 1>(1-1) osc. strengths

TABLE 14

OSCILLATOR STRENGTH FOR FREE-FREE TRANSITIONS

NEON-LIKE ALUMINUM

ELECTRON DENSITY=2.2E+23 TEMP=50 EV

PHOTON ENERGY=0.370 AT.UNIT

E(INCIDENT) (AT.UNIT)	E(OUTGOING) (AT.UNIT)	OSCILLATOR STRENGTH * (AT.UNIT)
1.00	1.370	0.1935E+02
2.00	2.370	0.4743E+02
5.00	5.370	0.9232E+02
10.00	10.370	0.1555E+03
15.00	15.370	0.2325E+03
20.00	20.370	0.3208E+03
25.00	25.370	0.4189E+03
30.00	30.370	0.5254E+03
50.00	50.370	0.6574E+03
70.00	70.370	0.8069E+03
100.00	100.370	0.9744E+03
150.00	150.370	0.1160E+04
200.00	200.370	0.1357E+04

\* Sum of  $l>(l+1)$  osc. strengths

TABLE 15

OSCILLATOR STRENGTH FOR FREE-FREE TRANSITONS

NEON-LIKE ALUMINUM

ELECTRON DENSITY=2.2E+23 TEMP=50 EV

PHOTON ENERGY=0.740 AT.UNIT

E(INCIDENT) (AT.UNIT)	E(OUTGOING) (AT.UNIT)	OSCILLATOR STRENGTH * (AT.UNIT)
1.00	1.740	0.1917E+00
2.00	2.740	0.7512E+00
5.00	5.740	0.2469E+01
10.00	10.740	0.5598E+01
15.00	15.740	0.9739E+01
20.00	20.740	0.1467E+02
25.00	25.740	0.2024E+02
30.00	30.740	0.2635E+02
50.00	50.740	0.3402E+02
70.00	70.740	0.4269E+02
100.00	100.740	0.5237E+02
150.00	150.740	0.6304E+02
200.00	200.740	0.7429E+02

\* Sum of 1>(1-1) osc. strengths

TABLE 16

OSCILLATOR STRENGTH FOR FREE-FREE TRANSITIONS

NEON-LIKE ALUMINUM

ELECTRON DENSITY=2.2E+23 TEMP=50 EV

PHOTON ENERGY=0.740 AT.UNIT

E(INCIDENT) (AT.UNIT)	E(OUTGOING) (AT.UNIT)	OSCILLATOR STRENGTH * (AT.UNIT)
1.00	1.740	0.4742E+01
2.00	2.740	0.1021E+02
5.00	5.740	0.1734E+02
10.00	10.740	0.2646E+02
15.00	15.740	0.3713E+02
20.00	20.740	0.4911E+02
25.00	25.740	0.6223E+02
30.00	30.740	0.7634E+02
50.00	50.740	= 0.9347E+02
70.00	70.740	0.1127E+03
100.00	100.740	0.1340E+03
150.00	150.740	0.1576E+03
200.00	200.740	0.1825E+03

\* Sum of  $l>(1+1)$  osc. strengths

TABLE 17

OSCILLATOR STRENGTH FOR FREE-FREE TRANSITIONS

NEON-LIKE ALUMINUM

ELECTRON DENSITY=2.2E+23 TEMP=50 EV

PHOTON ENERGY=1.295 AT.UNIT

E(INCIDENT) (AT.UNIT)	E(OUTGOING) (AT.UNIT)	OSCILLATOR STRENGTH * (AT.UNIT)
1.00	2.295	0.4104E-01
2.00	3.295	0.1223E+00
5.00	6.295	0.3603E+00
10.00	11.295	0.8347E+00
15.00	16.295	0.1495E+01
20.00	21.295	0.2304E+01
25.00	26.295	0.3238E+01
30.00	31.295	0.4277E+01
50.00	51.295	$\approx$ 0.5621E+01
70.00	71.295	0.7164E+01
100.00	101.295	0.8907E+01
150.00	151.295	0.1085E+02
200.00	201.295	0.1291E+02

\* Sum of  $l>(l-1)$  osc. strengths

TABLE 18

OSCILLATOR STRENGTH FOR FREE-FREE TRANSITIONS

NEON-LIKE ALUMINUM

ELECTRON DENSITY=2.2E+23 TEMP=50 EV

PHOTON ENERGY=1.295 AT.UNIT

E(INCIDENT) (AT.UNIT)	E(OUTGOING) (AT.UNIT)	OSCILLATOR STRENGTH * (AT.UNIT)
1.00	2.295	0.1552E+01
2.00	3.295	0.3140E+01
5.00	6.295	0.4921E+01
10.00	11.295	0.6979E+01
15.00	16.295	0.9278E+01
20.00	21.295	0.1179E+02
25.00	26.295	0.1448E+02
30.00	31.295	0.1734E+02
50.00	51.295	0.2072E+02
70.00	71.295	= 0.2446E+02
100.00	101.295	0.2857E+02
150.00	151.295	0.3306E+02
200.00	201.295	0.3778E+02

\* 1>(l+1) osc. strengths

TABLE 19

OSCILLATOR STRENGTH FOR FREE-FREE TRANSITIONS

NEON-LIKE ALUMINUM

ELECTRON DENSITY=2.2E+23 TEMP=50 EV

PHOTON ENERGY=2.220 AT.UNIT

E(INCIDENT) (AT.UNIT)	E(OUTGOING) (AT.UNIT)	OSCILLATOR STRENGTH * (AT.UNIT)
1.00	3.220	0.4791E+00
2.00	4.220	0.9546E+00
5.00	7.220	0.1449E+01
10.00	12.220	0.1976E+01
15.00	17.220	0.2535E+01
20.00	22.220	0.3126E+01
25.00	27.220	0.3745E+01
30.00	32.220	0.4391E+01
50.00	52.220	0.5123E+01
70.00	72.220	= 0.5915E+01
100.00	102.220	0.6772E+01
150.00	152.220	0.7696E+01
200.00	202.220	0.8659E+01

\* 1&gt;(l+1) osc. strengths

TABLE 20

OSCILLATOR STRENGTH FOR FREE-FREE TRANSITIONS

NEON-LIKE ALUMINUM

ELECTRON DENSITY=2.2E+23 TEMP=50 EV

PHOTON ENERGY=2.220 AT.UNIT

E(INCIDENT) (AT.UNIT)	E(OUTGOING) (AT.UNIT)	OSCILLATOR STRENGTH *
1.00	3.220	0.1293E-01
2.00	4.220	0.2996E-01
5.00	7.220	0.6580E-01
10.00	12.220	0.1374E+00
15.00	17.220	0.2416E+00
20.00	22.220	0.3740E+00
25.00	27.220	0.5308E+00
30.00	32.220	0.7088E+00
50.00	52.220	0.9500E+00
70.00	72.220	0.1233E+01
100.00	102.220	0.1559E+01
150.00	152.220	0.1929E+01
200.00	202.220	0.2324E+01

\* Sum of  $1>(l-1)$  osc. strengths

## STEP 1

$$Q = 0.00000E+00 \quad Q_1 = 0.00000E+00 \quad Q_2 = 0.00000E+00$$

$$\text{NORMALIZATION INTEGRAL} = 0.1000000E+01$$

$$\text{NORMALIZATION INTEGRAL} = 0.9999996E+00$$

$$\text{NORMALIZATION INTEGRAL} = 0.1000000E+01$$

$$EIN = C. 200000E+01 \quad GMEGA = 0. 370000E+00$$

$$X(L+1) = X(L-1) * X(L+1) ** 2 \quad L**X(L-1)**2$$

0	-0. 367936E+00	0. 000000E+00	0. 135414E+00	0. 000000E+00
1	-0. 421521E+00	-0. 366987E+00	0. 354634E+00	0. 134679E+00
2	-0. 370257E+00	-0. 342982E+00	0. 411274E+00	0. 235273E+00
3	-0. 25963CE+00	-0. 205677E+00	0. 230074E+00	0. 13063SE+00
4	-0. 174782E+00	-0. 107042E+00	0. 152744E+00	0. 458318E-01
5	-0. 135322E+00	-0. 453687E-01	0. 109672E+00	0. 213786E-01
6	-0. 107228E+00	-0. 413088E-01	0. 825133E-01	0. 112535E-01
7	-0. 908502E-01	-0. 304275E-01	0. 659575E-01	0. 646167E-02
8	-0. 769934E-01	-0. 242384E-01	0. 533602E-01	0. 402787E-02
9	-0. 641771E-01	-0. 171736E-01	0. 437740E-01	0. 265446E-02
10	-0. 574039E-01	-0. 125104E-01	0. 362472E-01	0. 182532E-02
11	-0. 501255E-01	-0. 108443E-01	0. 301507E-01	0. 129356E-02
12	-0. 437899E-01	-0. 823375E-02	0. 251564E-01	0. 736463E-03
13	-0. 367592E-01	-0. 717744E-02	0. 210307E-01	0. 468494E-03
14	-0. 342587E-01	-0. 604892E-02	0. 176049E-01	0. 312259E-03
15	-0. 303649E-01	-0. 506356E-02	0. 147528E-01	0. 264597E-03
16	-0. 269740E-01	-0. 426425E-02	0. 123694E-01	0. 220942E-03
17	-0. 240123E-01	-0. 360926E-02	0. 1013753E-01	0. 221457E-03
18	-0. 214147E-01	-0. 303677E-02	0. 871303E-02	0. 169512E-03
19	-0. 191258E-01	-0. 251951E-02	0. 731578E-02	0. 130376E-03
20	-0. 171024E-01	-0. 204236E-02	0. 614592E-02	0. 100678E-03
21	-0. 153223E-01	-0. 172874E-02	0. 512501E-02	0. 761209E-04
22	-0. 137232E-01	-0. 146242E-02	0. 434626E-02	0. 520603E-04
23	-0. 123581E-01	-0. 113671E-02	0. 365347E-02	0. 474661E-04
24	-0. 110276E-01	-0. 104318E-02	0. 307259E-02	0. 321951E-04
25	-0. 997522E-01	-0. 108654E-02	0. 2588713E-02	0. 251742E-04
26	-0. 397904E-01	-0. 740710E-03	0. 2175823E-02	0. 230603E-04
27	-0. 808563E-02	-0. 611754E-03	0. 163151E-02	0. 161751E-04
28	-0. 729201E-02	-0. 715883E-03	0. 154245E-02	0. 143492E-04
29	-0. 657642E-02	-0. 627900E-03	0. 129627E-02	0. 114697E-04
30	-0. 593767E-02	-0. 548210E-03	0. 107273E-02	0. 960261E-05

$$\text{SUM OF } (L+1)*X(L+1)**2 = 0. 165449E+01$$

$$\text{TOTAL SUM} = C. 246362E+01$$

$$\text{BETHE APPROXIMATION} = 0. 156016E+01$$

$$DF/DE = C. 116727E+04$$

$$EIN = C. 100000E+01 \quad GMEGA = 0. 370000E+00$$

0	-0. 777655E+00	0. 000000E+00	0. 601794E+00	0. 000000E+00
1	-0. 727424E+00	-0. 248374E+00	0. 165825E+01	0. 560662E+01
2	-0. 457162E+00	-0. 4665947E+00	0. 5255711E+01	0. 6632854E+01

Copyright 1984 by J. R. Gaskins  
All rights reserved. Reproduction  
in whole or in part is prohibited.

$EIN = C 3400000000$   
 $\text{DF/DE} = C 4222995E+01$   
 $\text{TOTAL SUM = C 4233581E+04}$   
 $\text{BETHE APPROXIMATION = C 2266694E+01}$   
 $\text{SUM OF (L+1)*(-1)^L * F(L) = C 2266694E+01}$   
 $\text{L = 1}$   
 $L+1 = 2$   
 $L+2 = 3$   
 $L+3 = 4$   
 $L+4 = 5$   
 $L+5 = 6$   
 $L+6 = 7$   
 $L+7 = 8$   
 $L+8 = 9$   
 $L+9 = 10$   
 $L+10 = 11$   
 $L+11 = 12$   
 $L+12 = 13$   
 $L+13 = 14$   
 $L+14 = 15$   
 $L+15 = 16$   
 $L+16 = 17$   
 $L+17 = 18$   
 $L+18 = 19$   
 $L+19 = 20$   
 $L+20 = 21$   
 $L+21 = 22$   
 $L+22 = 23$   
 $L+23 = 24$   
 $L+24 = 25$   
 $L+25 = 26$   
 $L+26 = 27$   
 $L+27 = 28$   
 $L+28 = 29$   
 $L+29 = 30$   
 $L+30 = 31$   
 $L+31 = 32$   
 $L+32 = 33$   
 $L+33 = 34$   
 $L+34 = 35$   
 $L+35 = 36$   
 $L+36 = 37$   
 $L+37 = 38$   
 $L+38 = 39$   
 $L+39 = 40$   
 $L+40 = 41$   
 $L+41 = 42$   
 $L+42 = 43$   
 $L+43 = 44$   
 $L+44 = 45$   
 $L+45 = 46$   
 $L+46 = 47$   
 $L+47 = 48$   
 $L+48 = 49$   
 $L+49 = 50$   
 $L+50 = 51$   
 $L+51 = 52$   
 $L+52 = 53$   
 $L+53 = 54$   
 $L+54 = 55$   
 $L+55 = 56$   
 $L+56 = 57$   
 $L+57 = 58$   
 $L+58 = 59$   
 $L+59 = 60$   
 $L+60 = 61$   
 $L+61 = 62$   
 $L+62 = 63$   
 $L+63 = 64$   
 $L+64 = 65$   
 $L+65 = 66$   
 $L+66 = 67$   
 $L+67 = 68$   
 $L+68 = 69$   
 $L+69 = 70$   
 $L+70 = 71$   
 $L+71 = 72$   
 $L+72 = 73$   
 $L+73 = 74$   
 $L+74 = 75$   
 $L+75 = 76$   
 $L+76 = 77$   
 $L+77 = 78$   
 $L+78 = 79$   
 $L+79 = 80$   
 $L+80 = 81$   
 $L+81 = 82$   
 $L+82 = 83$   
 $L+83 = 84$   
 $L+84 = 85$   
 $L+85 = 86$   
 $L+86 = 87$   
 $L+87 = 88$   
 $L+88 = 89$   
 $L+89 = 90$   
 $L+90 = 91$   
 $L+91 = 92$   
 $L+92 = 93$   
 $L+93 = 94$   
 $L+94 = 95$   
 $L+95 = 96$   
 $L+96 = 97$   
 $L+97 = 98$   
 $L+98 = 99$   
 $L+99 = 100$

$EIN = C 3400000000$   
 $\text{DF/DE} = C 4222995E+01$   
 $\text{TOTAL SUM = C 4233581E+04}$   
 $\text{BETHE APPROXIMATION = C 2266694E+01}$   
 $\text{SUM OF (L+1)*(-1)^L * F(L) = C 2266694E+01}$   
 $\text{L = 1}$   
 $L+1 = 2$   
 $L+2 = 3$   
 $L+3 = 4$   
 $L+4 = 5$   
 $L+5 = 6$   
 $L+6 = 7$   
 $L+7 = 8$   
 $L+8 = 9$   
 $L+9 = 10$   
 $L+10 = 11$   
 $L+11 = 12$   
 $L+12 = 13$   
 $L+13 = 14$   
 $L+14 = 15$   
 $L+15 = 16$   
 $L+16 = 17$   
 $L+17 = 18$   
 $L+18 = 19$   
 $L+19 = 20$   
 $L+20 = 21$   
 $L+21 = 22$   
 $L+22 = 23$   
 $L+23 = 24$   
 $L+24 = 25$   
 $L+25 = 26$   
 $L+26 = 27$   
 $L+27 = 28$   
 $L+28 = 29$   
 $L+29 = 30$   
 $L+30 = 31$   
 $L+31 = 32$   
 $L+32 = 33$   
 $L+33 = 34$   
 $L+34 = 35$   
 $L+35 = 36$   
 $L+36 = 37$   
 $L+37 = 38$   
 $L+38 = 39$   
 $L+39 = 40$   
 $L+40 = 41$   
 $L+41 = 42$   
 $L+42 = 43$   
 $L+43 = 44$   
 $L+44 = 45$   
 $L+45 = 46$   
 $L+46 = 47$   
 $L+47 = 48$   
 $L+48 = 49$   
 $L+49 = 50$   
 $L+50 = 51$   
 $L+51 = 52$   
 $L+52 = 53$   
 $L+53 = 54$   
 $L+54 = 55$   
 $L+55 = 56$   
 $L+56 = 57$   
 $L+57 = 58$   
 $L+58 = 59$   
 $L+59 = 60$   
 $L+60 = 61$   
 $L+61 = 62$   
 $L+62 = 63$   
 $L+63 = 64$   
 $L+64 = 65$   
 $L+65 = 66$   
 $L+66 = 67$   
 $L+67 = 68$   
 $L+68 = 69$   
 $L+69 = 70$   
 $L+70 = 71$   
 $L+71 = 72$   
 $L+72 = 73$   
 $L+73 = 74$   
 $L+74 = 75$   
 $L+75 = 76$   
 $L+76 = 77$   
 $L+77 = 78$   
 $L+78 = 79$   
 $L+79 = 80$   
 $L+80 = 81$   
 $L+81 = 82$   
 $L+82 = 83$   
 $L+83 = 84$   
 $L+84 = 85$   
 $L+85 = 86$   
 $L+86 = 87$   
 $L+87 = 88$   
 $L+88 = 89$   
 $L+89 = 90$   
 $L+90 = 91$   
 $L+91 = 92$   
 $L+92 = 93$   
 $L+93 = 94$   
 $L+94 = 95$   
 $L+95 = 96$   
 $L+96 = 97$   
 $L+97 = 98$   
 $L+98 = 99$   
 $L+99 = 100$

Copy available at NHC does not permit full reproduction

在於此，我們可以說，這就是「中國化」的「新儒學」。

DETERMINATION OF THE APPROXIMATE VALUE OF  $\pi$  BY THE CORDIC ALGORITHM

THE PRACTICAL USE OF THE BIBLIOGRAPHY OF THE BIBLE IN TEACHING THE BIBLE.

SPICA = 0.2000000E+00;

卷之三

-0	42422C+00	0	000000E+00
-0	516611E+00	-0	347700E+00
-0	453284E+00	-0	347241E+00
-0	246277E+00	-0	105670E+00
-0	179715E+00	-0	626900E+00
-0	130411E+00	-0	454030E+00
-0	979573E-01	-0	292539E+00
-0	758234E-01	-0	137783E+00
-0	558753E-01	-0	125734E+00
-0	480500E-01	-0	622565E+00
-0	388633E-01	-0	629648E+00
-0	314490E-01	-0	483019E+00
-0	259860E-01	-0	363795E+00
-0	212640E-01	-0	242611E+00
-0	175340E-01	-0	175340E+00

**Copy available in U.S.A. but not  
permits fully legal reproduction**

卷之三

STEP 2  
S 20000E-0.2 0.00000+00 0.00000E00

FIN = S 10000E+01 CMAX = S 100000E+00

L1 X(L1) X(L1+1) X(L1+2) X(L1+3) X(L1+4)

S -0.45628E+00  
-0.52576E+00  
-0.50113E+00  
-0.24492E+00  
-0.12895E+00  
-0.72132E-01  
-0.41435E-01  
-0.24385E-01  
-0.14561E-01  
-0.88104E-01  
-0.53607E-01  
-0.32778E-01  
-0.20114E-01  
-0.12380E-01  
-0.76350E-01  
-0.47233E-01  
TOTAL SUM = S 241192E+01  
BETHE APPROXIMATION = S 24120195E+01  
DF/RE = S 269047E-02

SUM OF (L+1)\*X(L+1)\*\*2 = S 0.249751E+02

FIN = S 20000E+01 CMAX = S 100000E+00

L1 X(L1) X(L1+1)

S -0.52417E+00  
-0.67851E+00  
-0.50369E+00  
-0.26862E+00  
-0.16225E+00  
-0.10486E+00  
-0.69785E+00  
-0.47754E+00  
-0.33359E+00  
-0.23645E+00  
-0.16237E+00  
-0.12524E+00  
-0.86777E+00  
-0.64704E+00  
-0.47355E+00  
-0.34275E+00  
-0.25534E+00  
-0.18062E+00  
-0.13587E+00  
-0.10230E+00  
-0.75527E+00  
-0.55822E+00  
-0.412657E+00  
-0.301445E+00

X(L1+2) X(L1+3) X(L1+4)

S 0.69200E+00  
-0.43219E+00  
-0.31344E+00  
-0.14897E+00  
-0.82034E+00  
-0.39760E+00  
-0.16724E+00  
-0.61462E+00  
-0.25175E+00  
-0.33656E+00  
-0.20651E+00  
-0.12146E+00  
-0.65536E+00  
-0.31675E+00  
-0.13647E+00  
-0.61771E+00  
-0.28668E+00  
-0.64562E+00  
-0.47317E+00  
-0.344671E+00  
-0.25465E+00  
-0.12545E+00  
-0.59153E+00

X(L1+5) X(L1+6) X(L1+7)

S 0.69200E+00  
-0.43219E+00  
-0.31344E+00  
-0.14897E+00  
-0.82034E+00  
-0.39760E+00  
-0.16724E+00  
-0.61462E+00  
-0.25175E+00  
-0.33656E+00  
-0.20651E+00  
-0.12146E+00  
-0.65536E+00  
-0.31675E+00  
-0.13647E+00  
-0.61771E+00  
-0.28668E+00  
-0.64562E+00  
-0.47317E+00  
-0.344671E+00  
-0.25465E+00  
-0.12545E+00  
-0.59153E+00



-0.159247E+01  
 -0.126324E+01  
 -0.103203E+01  
 -0.860705E+01  
 -0.720649E+01  
 -0.625082E+01  
 -0.541726E+01  
 -0.473764E+01  
 -0.417420E+01  
 -0.370291E+01  
 -0.330623E+01  
 -0.295507E+01  
 -0.265020E+01  
 -0.239462E+01  
 -0.216416E+01  
 -0.196056E+01  
 -0.177959E+01  
 -0.161792E+01  
 -0.147316E+01  
 -0.124577E+01  
 -0.122523E+01  
 -0.111930E+01  
 -0.102403E+01  
 -0.927294E+00  
 -0.853435E+00  
 -0.784522E+00  
 -0.721571E+00  
 -0.669271E+00  
 -0.605671E+00  
 -0.553860E+00  
 -0.513423E+00  
 -0.472647E+00  
 -0.434265E+00  
 -0.399447E+00  
 SUM OF ABSOLUTE VALUES = 6.63644E+01  
 TOTAL SUM = 6.45999E+01  
 BETHE APPROXIMATION = 6.20999E+01  
 DIFFERENCE = 6.20999E+01

EIN = C 2733334.147  
 \*MLT1  
 \*MLT2  
 \*MLT3  
 \*MLT4

0.111537E+01  
 -0.7086279E+00  
 -0.572170E+00  
 -0.351602E+00  
 -0.235566E+00  
 -0.173910E+00  
 -0.137325E+00  
 -0.113423E+00  
 -0.964033E+01  
 -0.834979E+01  
 -0.732647E+01  
 -0.650375E+01  
 -0.561577E+01  
 -0.524577E+01  
 -0.474177E+01

**Copy available but it does not  
permit fully legible reproduction**

SUM OF		TOTAL SUM -	
		BETHE OPTIMIZATION	DF/CE = 0.010000000000000000
15	-0 42365.3E-01	-0 12650.9E-01	0 393.91E-01
16	-0 37854.4E-01	-0 12795.9E-01	0 393.91E-01
17	-0 36734.8E-01	-0 11126.9E-01	0 393.91E-01
18	-0 35995.0E-01	-0 97482.6E-02	0 393.91E-01
19	-0 31524.1E-01	-0 36923.3E-02	0 393.91E-01
20	-0 27464.6E-01	-0 76154.4E-02	0 393.91E-01
21	-0 27415.2E-01	-0 62716.9E-02	0 393.91E-01
22	-0 25543.4E-01	-0 59163.4E-02	0 393.91E-01
23	-0 24041.3E-01	-0 52725.4E-02	0 393.91E-01
24	-0 22575.1E-01	-0 45443.1E-02	0 393.91E-01
25	-0 21227.4E-01	-0 43869.4E-02	0 393.91E-01
26	-0 20004.0E-01	-0 45772.4E-02	0 393.91E-01
27	-0 18845.6E-01	-0 42194.4E-02	0 393.91E-01
28	-0 17812.1E-01	-0 36122.3E-02	0 393.91E-01
29	-0 16324.0E-01	-0 31124.6E-02	0 393.91E-01
30	-0 15924.0E-01	-0 28467.3E-02	0 393.91E-01
31	-0 15073.5E-01	-0 24432.5E-02	0 393.91E-01
32	-0 14281.3E-01	-0 24349.1E-02	0 393.91E-01
33	-0 13521.3E-01	-0 24449.6E-02	0 393.91E-01
34	-0 12843.2E-01	-0 26611.9E-02	0 393.91E-01
35	-0 12149.4E-01	-0 28222.4E-02	0 393.91E-01
36	-0 11561.0E-01	-0 27951.2E-02	0 393.91E-01
37	-0 11004.4E-01	-0 16629.4E-02	0 393.91E-01
38	-0 10461.1E-01	-0 11436.4E-02	0 393.91E-01

25 -0. 246535E+01 -0. 491730E+02  
 26 -0. 234252E+01 -0. 635220E+02  
 27 -0. 222519E+01 -0. 585075E+02  
 28 -0. 212424E+01 -0. 540559E+02  
 29 -0. 202649E+01 -0. 500527E+02  
 30 -0. 193570E+01 -0. 464529E+02  
 31 -0. 185090E+01 -0. 430559E+02  
 32 -0. 177144E+01 -0. 402951E+02  
 33 -0. 167633E+01 -0. 376358E+02  
 34 -0. 162525E+01 -0. 352821E+02  
 35 -0. 155950E+01 -0. 324923E+02  
 36 -0. 149674E+01 -0. 299496E+02  
 37 -0. 143775E+01 -0. 2769738E+02  
 38 -0. 138105E+01 -0. 257265E+02  
 SUM OF CL+1 MAX +1.0\*E-01 = 0. 674703E+01  
 TOTAL SUM = 0. 669130E+01  
 BETHE APPROXIMATION = 0. 669130E+01  
 DF/DE = 0. 2098430E+00

$EIN = C \cdot \text{SIN}(C \cdot DE)$

$L = 10^{(1+10) \cdot DE}$        $\text{DECA} = 0. 1462002 \cdot 10^4$   
 0. 147677E+01 0. 966630E+00 0. 216534E+01  
 -0. 771221E+00 -0. 137177E+01 0. 186534E+01  
 -0. 610573E+00 -0. 675562E+00 0. 112565E+01  
 -0. 405350E+00 -0. 526924E+00 0. 657713E+00  
 -0. 263546E+00 -0. 338433E+00 0. 461085E+00  
 -0. 208274E+00 -0. 277133E+00 0. 260423E+00  
 -0. 160519E+00 -0. 157244E+00 0. 180545E+00  
 -0. 127053E+00 -0. 114671E+00 0. 132449E+00  
 -0. 107523E+00 -0. 891393E+00 0. 146692E+00  
 -0. 721462E+00 -0. 596823E+00 0. 642632E+00  
 10 -0. 866923E+01 -0. 3735137E+01 0. 715232E+01  
 11 -0. 718201E+01 -0. 484731E+01 0. 613279E+01  
 12 -0. 642113E+01 0. 414551E+01 0. 564531E+01  
 13 -0. 583544E+01 -0. 759677E+01 0. 464475E+01  
 14 -0. 538267E+01 0. 541999E+01 0. 435291E+01  
 15 -0. 477432E+01 -0. 229511E+01 0. 365494E+01  
 16 -0. 460514E+01 -0. 173722E+01 0. 260507E+01  
 17 -0. 423462E+01 -0. 126255E+01 0. 205363E+01  
 18 -0. 400514E+01 0. 155353E+01 0. 164385E+01  
 19 -0. 375532E+01 0. 169534E+01 0. 202666E+01  
 20 -0. 353264E+01 -0. 143452E+01 0. 236273E+01  
 21 -0. 333305E+01 -0. 146374E+01 0. 244423E+01  
 22 -0. 315333E+01 0. 135942E+01 0. 228779E+01  
 23 -0. 292035E+01 0. 155351E+01 0. 214423E+01  
 24 -0. 264332E+01 -0. 114601E+01 0. 202112E+01  
 25 -0. 227233E+01 -0. 165232E+01 0. 146253E+01  
 26 -0. 216359E+01 -0. 979336E+00 0. 160553E+01  
 27 -0. 202931E+01 -0. 768328E+00 0. 171711E+01  
 28 -0. 194944E+01 -0. 649913E+00 0. 182211E+01  
 29 -0. 183139E+01 -0. 529211E+00 0. 193411E+01

-0 18445E-01  
 -0 17644E-01  
 -0 16735E-01  
 -0 16442E-01  
 SUM OF C4 = 0.44444E-01  
 TOTAL SUM = 0.37644E-01  
 BETTER APPROXIMATION = 0.37644E-01  
 OFFICE = 0.20122E+00  
 STEPS = 12121  
 EQUATION = 0.00000E+00

卷之三

卷之三

卷之三

卷之三

卷之三

123669SE-001 10 187149E-001

卷之三

卷之三

卷之三

THE BOSTONIAN 1849

卷之三

卷之三

卷之三

卷之三

-0.258455E+00 -0.1228671E+00

0 23196974 0 411398 01 0 215401E-01

卷之三

0 -0.807326E-02 -0.706641E-02

08-34688CE-03  
08-34688CE-04  
08-34688CE-05  
08-34688CE-06  
08-34688CE-07  
08-34688CE-08  
08-34688CE-09

卷之三

*Copy available by interlibrary loan  
Permit fully legal reproduction*

100,000,000 = 100,000,000

Copy available - FID date not  
permit fully legible reproduction

10 115173E+00  
-0 957279E-01  
-0 827103E-01

10 715185E-01  
-0 626645E-01

-0 552603E-01  
-0 490213E-01

-0 459444E-01  
-0 391379E-01

-0 355973E-01  
-0 322233E-01

-0 293333E-01  
-0 267363E-01

-0 245273E-01  
-0 220474E-01

-0 202235E-01  
-0 181936E-01

-0 175615E-01  
-0 163142E-01

-0 151305E-01  
-0 140366E-01

-0 132345E-01  
-0 121170E-01

-0 112343E-01  
-0 104363E-01

-0 975324E-01  
-0 912363E-01

-0 851135E-01  
-0 794857E-01

-0 742503E-01  
-0 693933E-01

-0 646833E-01  
SUM OF ((1+1)\*X(1+1)\*X2 = C 610479E+01

TOTAL SUM = C 504356E+01  
BETHE APPROXIMANT = C 121872E+01  
OF/CE = 2 326711E461

11 623623E-01  
-0 541953E-01  
-0 342135E-01

10 267723E-01  
-0 231312E-01

-0 192232E-01  
-0 153831E-01

-0 125231E-01  
-0 95931E-01

-0 684435E-01  
-0 474455E-01

-0 355834E-01  
-0 303935E-01

-0 253835E-01  
-0 207363E-01

-0 181585E-01  
-0 167647E-01

-0 150395E-01  
-0 140396E-01

-0 132396E-01  
-0 124497E-01

-0 116598E-01  
-0 110699E-01

-0 104613E-01  
-0 987413E-01

-0 928333E-01  
-0 874333E-01

-0 827442E-01  
-0 765845E-01

-0 724455E-01  
-0 674466E-01

-0 634477E-01  
-0 594488E-01

-0 554499E-01  
-0 514510E-01

-0 474511E-01  
-0 434512E-01

-0 394513E-01  
-0 354514E-01

-0 314515E-01  
-0 274516E-01

-0 234517E-01  
-0 194518E-01

-0 154519E-01  
-0 114520E-01

-0 744521E-01  
-0 344522E-01

-0 144523E-01  
-0 744524E-01

-0 344525E-01  
-0 144526E-01

12 614903E-01  
-0 553133E-01

13 -0 500579E-01  
-0 455404E-01

14 -0 416334E-01  
-0 345335E-01

15 -0 306336E-01  
-0 246337E-01

16 -0 196338E-01  
-0 146339E-01

17 -0 106340E-01  
-0 763410E-01

18 -0 663412E-01  
-0 463413E-01

19 -0 363414E-01  
-0 263415E-01

20 -0 163416E-01  
-0 113417E-01

21 -0 663418E-01  
-0 463419E-01

22 -0 263420E-01  
-0 163421E-01

23 -0 106322E-01  
-0 763232E-01

24 -0 463233E-01  
-0 363234E-01

25 -0 206325E-01  
-0 166326E-01

26 -0 866327E-01  
-0 706328E-01

27 -0 366329E-01  
-0 266330E-01

28 -0 1466331E-01  
-0 1066332E-01

29 -0 5666333E-01  
-0 4266334E-01

30 -0 2266335E-01  
-0 1666336E-01

31 -0 8266337E-01  
-0 6266338E-01

32 -0 3266339E-01  
-0 2266340E-01

33 -0 1266341E-01  
-0 9266342E-01

34 -0 4666343E-01  
-0 3266344E-01

35 -0 1666345E-01  
-0 1266346E-01

36 -0 6266347E-01  
-0 4266348E-01

10 121872E+01

11 -0 668465E-01  
-0 514510E-01

12 -0 614903E-01  
-0 553133E-01

13 -0 500579E-01  
-0 455404E-01

14 -0 416334E-01  
-0 345335E-01

15 -0 306336E-01  
-0 246337E-01

16 -0 196338E-01  
-0 146339E-01

17 -0 106340E-01  
-0 763410E-01

18 -0 663412E-01  
-0 463413E-01

19 -0 363414E-01  
-0 263415E-01

20 -0 163416E-01  
-0 113417E-01

21 -0 663418E-01  
-0 463419E-01

22 -0 263420E-01  
-0 163421E-01

23 -0 106322E-01  
-0 763232E-01

24 -0 463233E-01  
-0 363234E-01

25 -0 206325E-01  
-0 166326E-01

26 -0 866327E-01  
-0 706328E-01

27 -0 366329E-01  
-0 266330E-01

28 -0 1466331E-01  
-0 1066332E-01

29 -0 5666333E-01  
-0 4266334E-01

30 -0 2266335E-01  
-0 1666336E-01

31 -0 8266337E-01  
-0 6266338E-01

32 -0 3266339E-01  
-0 2266340E-01

33 -0 1266341E-01  
-0 9266342E-01

34 -0 4666343E-01  
-0 3266344E-01

10 121872E+01

11 -0 668465E-01  
-0 514510E-01

12 -0 614903E-01  
-0 553133E-01

13 -0 500579E-01  
-0 455404E-01

14 -0 416334E-01  
-0 345335E-01

15 -0 306336E-01  
-0 246337E-01

16 -0 196338E-01  
-0 146339E-01

17 -0 106340E-01  
-0 763410E-01

18 -0 663412E-01  
-0 463413E-01

19 -0 363414E-01  
-0 263415E-01

20 -0 163416E-01  
-0 113417E-01

21 -0 663418E-01  
-0 463419E-01

22 -0 263420E-01  
-0 163421E-01

23 -0 106322E-01  
-0 763232E-01

24 -0 463233E-01  
-0 363234E-01

25 -0 206325E-01  
-0 166326E-01

26 -0 866327E-01  
-0 706328E-01

27 -0 366329E-01  
-0 266330E-01

28 -0 1466331E-01  
-0 1066332E-01

29 -0 5666333E-01  
-0 4266334E-01

30 -0 2266335E-01  
-0 1666336E-01

31 -0 8266337E-01  
-0 6266338E-01

32 -0 3266339E-01  
-0 2266340E-01

33 -0 1266341E-01  
-0 9266342E-01

34 -0 4666343E-01  
-0 3266344E-01

10 121872E+01

11 -0 668465E-01  
-0 514510E-01

12 -0 614903E-01  
-0 553133E-01

13 -0 500579E-01  
-0 455404E-01

14 -0 416334E-01  
-0 345335E-01

15 -0 306336E-01  
-0 246337E-01

16 -0 196338E-01  
-0 146339E-01

17 -0 106340E-01  
-0 763410E-01

18 -0 663412E-01  
-0 463413E-01

19 -0 363414E-01  
-0 263415E-01

20 -0 163416E-01  
-0 113417E-01

21 -0 663418E-01  
-0 463419E-01

22 -0 263420E-01  
-0 163421E-01

23 -0 106322E-01  
-0 763232E-01

24 -0 463233E-01  
-0 363234E-01

25 -0 206325E-01  
-0 166326E-01

26 -0 866327E-01  
-0 706328E-01

27 -0 366329E-01  
-0 266330E-01

28 -0 1466331E-01  
-0 1066332E-01

29 -0 5666333E-01  
-0 4266334E-01

30 -0 2266335E-01  
-0 1666336E-01

31 -0 8266337E-01  
-0 6266338E-01

32 -0 3266339E-01  
-0 2266340E-01

33 -0 1266341E-01  
-0 9266342E-01

34 -0 4666343E-01  
-0 3266344E-01

10 121872E+01

11 -0 668465E-01  
-0 514510E-01

12 -0 614903E-01  
-0 553133E-01

13 -0 500579E-01  
-0 455404E-01

14 -0 416334E-01  
-0 345335E-01

15 -0 306336E-01  
-0 246337E-01

16 -0 196338E-01  
-0 146339E-01

17 -0 106340E-01  
-0 763410E-01

18 -0 663412E-01  
-0 463413E-01

19 -0 363414E-01  
-0 263415E-01

20 -0 163416E-01  
-0 113417E-01

21 -0 663418E-01  
-0 463419E-01

22 -0 263420E-01  
-0 163421E-01

23 -0 106322E-01  
-0 763232E-01

24 -0 463233E-01  
-0 363234E-01

25 -0 206325E-01  
-0 166326E-01

26 -0 866327E-01  
-0 706328E-01

27 -0 366329E-01  
-0 266330E-01

28 -0 1466331E-01  
-0 1066332E-01

29 -0 5666333E-01  
-0 4266334E-01

30 -0 2266335E-01  
-0 1666336E-01

31 -0 8266337E-01  
-0 6266338E-01

32 -0 3266339E-01  
-0 2266340E-01

33 -0 1266341E-01  
-0 9266342E-01

34 -0 4666343E-01  
-0 3266344E-01

10 121872E+01

11 -0 668465E-01  
-0 514510E-01

12 -0 614903E-01  
-0 553133E-01

13 -0 500579E-01  
-0 455404E-01

14 -0 416334E-01  
-0 345335E-01

15 -0 306336E-01  
-0 246337E-01

16 -0 196338E-01  
-0 146339E-01

17 -0 106340E-01  
-0 763410E-01

18 -0 663412E-01  
-0 463413E-01

19 -0 363414E-01  
-0 263415E-01

20 -0 163416E-01  
-0 113417E-01

21 -0 663418E-01  
-0 463419E-01

22 -0 263420E-01  
-0 163421E-01

23 -0 106322E-01  
-0

17

-0.282091E+01

-0.356911E+01

-0.3215E+01

-0.301629E+01

-0.265044E+01

-0.241807E+01

-0.241723E+01

-0.227255E+01

-0.215609E+01

-0.204531E+01

-0.194444E+01

-0.184357E+01

-0.174270E+01

-0.164183E+01

-0.154096E+01

-0.144009E+01

-0.133922E+01

-0.123835E+01

-0.113748E+01

-0.103661E+01

-0.935774E+01

-0.834887E+01

-0.734000E+01

-0.633113E+01

-0.532226E+01

-0.431339E+01

-0.330452E+01

-0.229565E+01

-0.128678E+01

-0.027791E+01

-0.000000E+00

18

-0.150317E+01

-0.995034E+01

-0.622731E+01

-0.413305E+01

-0.253401E+01

-0.215975E+01

-0.166553E+01

-0.111502E+01

-0.753945E+01

-0.633269E+01

-0.727725E+01

-0.664154E+01

-0.606634E+01

-0.547507E+01

-0.504425E+01

-0.465309E+01

-0.421612E+01

-0.360640E+01

-0.291124E+01

-0.272245E+01

-0.242471E+01

-0.212698E+01

-0.182925E+01

-0.153252E+01

-0.123579E+01

-0.093906E+01

-0.064233E+01

-0.034560E+01

-0.004887E+01

-0.000000E+00

19

-0.150317E+01

-0.995034E+01

-0.622731E+01

-0.413305E+01

-0.253401E+01

-0.215975E+01

-0.166553E+01

-0.111502E+01

-0.753945E+01

-0.633269E+01

-0.727725E+01

-0.664154E+01

-0.606634E+01

-0.547507E+01

-0.504425E+01

-0.465309E+01

-0.421612E+01

-0.360640E+01

-0.291124E+01

-0.272245E+01

-0.242471E+01

-0.212698E+01

-0.182925E+01

-0.153252E+01

-0.123579E+01

-0.093906E+01

-0.064233E+01

-0.034560E+01

-0.004887E+01

-0.000000E+00

20

-0.150317E+01

-0.995034E+01

-0.622731E+01

-0.413305E+01

-0.253401E+01

-0.215975E+01

-0.166553E+01

-0.111502E+01

-0.753945E+01

-0.633269E+01

-0.727725E+01

-0.664154E+01

-0.606634E+01

-0.547507E+01

-0.504425E+01

-0.465309E+01

-0.421612E+01

-0.360640E+01

-0.291124E+01

-0.272245E+01

-0.242471E+01

-0.212698E+01

-0.182925E+01

-0.153252E+01

-0.123579E+01

-0.093906E+01

-0.064233E+01

-0.034560E+01

-0.004887E+01

-0.000000E+00

21

-0.150317E+01

-0.995034E+01

-0.622731E+01

-0.413305E+01

-0.253401E+01

-0.215975E+01

-0.166553E+01

-0.111502E+01

-0.753945E+01

-0.633269E+01

-0.727725E+01

-0.664154E+01

-0.606634E+01

-0.547507E+01

-0.504425E+01

-0.465309E+01

-0.421612E+01

-0.360640E+01

-0.291124E+01

-0.272245E+01

-0.242471E+01

-0.212698E+01

-0.182925E+01

-0.153252E+01

-0.123579E+01

-0.093906E+01

-0.064233E+01

-0.034560E+01

-0.004887E+01

-0.000000E+00

22

-0.150317E+01

-0.995034E+01

-0.622731E+01

-0.413305E+01

-0.253401E+01

-0.215975E+01

-0.166553E+01

-0.111502E+01

-0.753945E+01

-0.633269E+01

-0.727725E+01

-0.664154E+01

-0.606634E+01

-0.547507E+01

-0.504425E+01

-0.465309E+01

-0.421612E+01

-0.360640E+01

-0.291124E+01

-0.272245E+01

-0.242471E+01

-0.212698E+01

-0.182925E+01

-0.153252E+01

-0.123579E+01

-0.093906E+01

-0.064233E+01

-0.034560E+01

-0.004887E+01

-0.000000E+00

23

-0.150317E+01

-0.995034E+01

-0.622731E+01

-0.413305E+01

-0.253401E+01

-0.215975E+01

-0.166553E+01

-0.111502E+01

-0.753945E+01

-0.633269E+01

-0.727725E+01

-0.664154E+01

-0.606634E+01

-0.547507E+01

-0.504425E+01

-0.465309E+01

-0.421612E+01

-0.360640E+01

-0.291124E+01

-0.272245E+01

-0.242471E+01

-0.212698E+01

-0.182925E+01

-0.153252E+01

-0.123579E+01

-0.093906E+01

-0.064233E+01

-0.034560E+01

-0.004887E+01

-0.000000E+00

24

-0.150317E+01

-0.995034E+01

-0.622731E+01

-0.413305E+01

-0.253401E+01

-0.215975E+01

-0.166553E+01

-0.111502E+01

-0.753945E+01

-0.633269E+01

-0.727725E+01

-0.664154E+01

-0.606634E+01

-0.547507E+01

-0.504425E+01

-0.465309E+01

-0.421612E+01

-0.360640E+01

-0.291124E+01

-0.272245E+01

-0.242471E+01

-0.212698E+01

-0.182925E+01

-0.153252E+01

-0.123579E+01

-0.093906E+01

-0.064233E+01

-0.034560E+01

-0.004887E+01

-0.000000E+00

25

-0.150317E+01

-0.995034E+01

-0.622731E+01

-0.413305E+01

-0.253401E+01

-0.215975E+01

-0.166553E+01

-0.111502E+01

-0.753945E+01

-0.633269E+01

-0.727725

**Copy available in 1970; does not permit fully reliable reproduction**

10 23.35 2.0  
 10 22.85 2.0  
 10 21.34 2.0  
 10 20.83 2.0  
 10 19.32 2.0  
 10 18.30 2.0  
 10 17.34 2.0  
 10 17.11 2.0  
 10 16.42 2.0  
 10 15.80 2.0  
 10 15.16 2.0  
 10 14.58 2.0  
 10 14.00 2.0  
 10 13.42 2.0  
 10 12.84 2.0  
 10 12.26 2.0  
 10 11.68 2.0  
 10 11.10 2.0  
 10 10.52 2.0  
 10 9.94 2.0  
 10 9.36 2.0  
 10 8.78 2.0  
 10 8.20 2.0  
 10 7.62 2.0  
 10 7.04 2.0  
 10 6.46 2.0  
 10 5.88 2.0  
 10 5.30 2.0  
 10 4.72 2.0  
 10 4.14 2.0  
 10 3.56 2.0  
 10 3.00 2.0  
 10 2.42 2.0  
 10 1.84 2.0  
 10 1.26 2.0  
 10 0.68 2.0  
 10 0.10 2.0  
 10 -0.38 2.0  
 10 -0.96 2.0  
 10 -1.54 2.0  
 10 -2.12 2.0  
 10 -2.70 2.0  
 10 -3.28 2.0  
 10 -3.86 2.0  
 10 -4.44 2.0  
 10 -5.02 2.0  
 10 -5.60 2.0  
 10 -6.18 2.0  
 10 -6.76 2.0  
 10 -7.34 2.0  
 10 -7.92 2.0  
 10 -8.50 2.0  
 10 -9.08 2.0  
 10 -9.66 2.0  
 10 -10.24 2.0  
 10 -10.82 2.0  
 10 -11.40 2.0  
 10 -11.98 2.0  
 10 -12.56 2.0  
 10 -13.14 2.0  
 10 -13.72 2.0  
 10 -14.30 2.0  
 10 -14.88 2.0  
 10 -15.46 2.0  
 10 -16.04 2.0  
 10 -16.62 2.0  
 10 -17.20 2.0  
 10 -17.78 2.0  
 10 -18.36 2.0  
 10 -18.94 2.0  
 10 -19.52 2.0  
 10 -20.10 2.0  
 10 -20.68 2.0  
 10 -21.26 2.0  
 10 -21.84 2.0  
 10 -22.42 2.0  
 10 -23.00 2.0  
 10 -23.58 2.0  
 10 -24.16 2.0  
 10 -24.74 2.0  
 10 -25.32 2.0  
 10 -25.90 2.0  
 10 -26.48 2.0  
 10 -27.06 2.0  
 10 -27.64 2.0  
 10 -28.22 2.0  
 10 -28.80 2.0  
 10 -29.38 2.0  
 10 -29.96 2.0  
 10 -30.54 2.0  
 10 -31.12 2.0  
 10 -31.70 2.0  
 10 -32.28 2.0  
 10 -32.86 2.0  
 10 -33.44 2.0  
 10 -34.02 2.0  
 10 -34.60 2.0  
 10 -35.18 2.0  
 10 -35.76 2.0  
 10 -36.34 2.0  
 10 -36.92 2.0  
 10 -37.50 2.0  
 10 -38.08 2.0  
 10 -38.66 2.0  
 10 -39.24 2.0  
 10 -39.82 2.0  
 10 -40.40 2.0  
 10 -40.98 2.0  
 10 -41.56 2.0  
 10 -42.14 2.0  
 10 -42.72 2.0  
 10 -43.30 2.0  
 10 -43.88 2.0  
 10 -44.46 2.0  
 10 -45.04 2.0  
 10 -45.62 2.0  
 10 -46.20 2.0  
 10 -46.78 2.0  
 10 -47.36 2.0  
 10 -47.94 2.0  
 10 -48.52 2.0  
 10 -49.10 2.0  
 10 -49.68 2.0  
 10 -50.26 2.0  
 10 -50.84 2.0  
 10 -51.42 2.0  
 10 -51.99 2.0  
 10 -52.57 2.0  
 10 -53.15 2.0  
 10 -53.73 2.0  
 10 -54.31 2.0  
 10 -54.89 2.0  
 10 -55.47 2.0  
 10 -56.05 2.0  
 10 -56.63 2.0  
 10 -57.21 2.0  
 10 -57.79 2.0  
 10 -58.37 2.0  
 10 -58.95 2.0  
 10 -59.53 2.0  
 10 -60.11 2.0  
 10 -60.69 2.0  
 10 -61.27 2.0  
 10 -61.85 2.0  
 10 -62.43 2.0  
 10 -63.01 2.0  
 10 -63.59 2.0  
 10 -64.17 2.0  
 10 -64.75 2.0  
 10 -65.33 2.0  
 10 -65.91 2.0  
 10 -66.49 2.0  
 10 -67.07 2.0  
 10 -67.65 2.0  
 10 -68.23 2.0  
 10 -68.81 2.0  
 10 -69.39 2.0  
 10 -69.97 2.0  
 10 -70.55 2.0  
 10 -71.13 2.0  
 10 -71.71 2.0  
 10 -72.29 2.0  
 10 -72.87 2.0  
 10 -73.45 2.0  
 10 -74.03 2.0  
 10 -74.61 2.0  
 10 -75.19 2.0  
 10 -75.77 2.0  
 10 -76.35 2.0  
 10 -76.93 2.0  
 10 -77.51 2.0  
 10 -78.09 2.0  
 10 -78.67 2.0  
 10 -79.25 2.0  
 10 -79.83 2.0  
 10 -80.41 2.0  
 10 -80.99 2.0  
 10 -81.57 2.0  
 10 -82.15 2.0  
 10 -82.73 2.0  
 10 -83.31 2.0  
 10 -83.89 2.0  
 10 -84.47 2.0  
 10 -85.05 2.0  
 10 -85.63 2.0  
 10 -86.21 2.0  
 10 -86.79 2.0  
 10 -87.37 2.0  
 10 -87.95 2.0  
 10 -88.53 2.0  
 10 -89.11 2.0  
 10 -89.69 2.0  
 10 -90.27 2.0  
 10 -90.85 2.0  
 10 -91.43 2.0  
 10 -91.01 2.0  
 10 -91.59 2.0  
 10 -92.17 2.0  
 10 -92.75 2.0  
 10 -93.33 2.0  
 10 -93.91 2.0  
 10 -94.49 2.0  
 10 -95.07 2.0  
 10 -95.65 2.0  
 10 -96.23 2.0  
 10 -96.81 2.0  
 10 -97.39 2.0  
 10 -97.97 2.0  
 10 -98.55 2.0  
 10 -99.13 2.0  
 10 -99.71 2.0  
 10 -100.29 2.0  
 10 -100.87 2.0  
 10 -101.45 2.0  
 10 -102.03 2.0  
 10 -102.61 2.0  
 10 -103.19 2.0  
 10 -103.77 2.0  
 10 -104.35 2.0  
 10 -104.93 2.0  
 10 -105.51 2.0  
 10 -106.09 2.0  
 10 -106.67 2.0  
 10 -107.25 2.0  
 10 -107.83 2.0  
 10 -108.41 2.0  
 10 -108.99 2.0  
 10 -109.57 2.0  
 10 -110.15 2.0  
 10 -110.73 2.0  
 10 -111.31 2.0  
 10 -111.89 2.0  
 10 -112.47 2.0  
 10 -113.05 2.0  
 10 -113.63 2.0  
 10 -114.21 2.0  
 10 -114.79 2.0  
 10 -115.37 2.0  
 10 -115.95 2.0  
 10 -116.53 2.0  
 10 -117.11 2.0  
 10 -117.69 2.0  
 10 -118.27 2.0  
 10 -118.85 2.0  
 10 -119.43 2.0  
 10 -120.01 2.0  
 10 -120.59 2.0  
 10 -121.17 2.0  
 10 -121.75 2.0  
 10 -122.33 2.0  
 10 -122.91 2.0  
 10 -123.49 2.0  
 10 -124.07 2.0  
 10 -124.65 2.0  
 10 -125.23 2.0  
 10 -125.81 2.0  
 10 -126.39 2.0  
 10 -126.97 2.0  
 10 -127.55 2.0  
 10 -128.13 2.0  
 10 -128.71 2.0  
 10 -129.29 2.0  
 10 -129.87 2.0  
 10 -130.45 2.0  
 10 -131.03 2.0  
 10 -131.61 2.0  
 10 -132.19 2.0  
 10 -132.77 2.0  
 10 -133.35 2.0  
 10 -133.93 2.0  
 10 -134.51 2.0  
 10 -135.09 2.0  
 10 -135.67 2.0  
 10 -136.25 2.0  
 10 -136.83 2.0  
 10 -137.41 2.0  
 10 -137.99 2.0  
 10 -138.57 2.0  
 10 -139.15 2.0  
 10 -139.73 2.0  
 10 -140.31 2.0  
 10 -140.89 2.0  
 10 -141.47 2.0  
 10 -142.05 2.0  
 10 -142.63 2.0  
 10 -143.21 2.0  
 10 -143.79 2.0  
 10 -144.37 2.0  
 10 -144.95 2.0  
 10 -145.53 2.0  
 10 -146.11 2.0  
 10 -146.69 2.0  
 10 -147.27 2.0  
 10 -147.85 2.0  
 10 -148.43 2.0  
 10 -148.01 2.0  
 10 -148.59 2.0  
 10 -149.17 2.0  
 10 -149.75 2.0  
 10 -150.33 2.0  
 10 -150.91 2.0  
 10 -151.49 2.0  
 10 -151.97 2.0  
 10 -152.55 2.0  
 10 -153.13 2.0  
 10 -153.71 2.0  
 10 -154.29 2.0  
 10 -154.87 2.0  
 10 -155.45 2.0  
 10 -156.03 2.0  
 10 -156.61 2.0  
 10 -157.19 2.0  
 10 -157.77 2.0  
 10 -158.35 2.0  
 10 -158.93 2.0  
 10 -159.51 2.0  
 10 -160.09 2.0  
 10 -160.67 2.0  
 10 -161.25 2.0  
 10 -161.83 2.0  
 10 -162.41 2.0  
 10 -162.99 2.0  
 10 -163.57 2.0  
 10 -164.15 2.0  
 10 -164.73 2.0  
 10 -165.31 2.0  
 10 -165.89 2.0  
 10 -166.47 2.0  
 10 -167.05 2.0  
 10 -167.63 2.0  
 10 -168.21 2.0  
 10 -168.79 2.0  
 10 -169.37 2.0  
 10 -169.95 2.0  
 10 -170.53 2.0  
 10 -171.11 2.0  
 10 -171.69 2.0  
 10 -172.27 2.0  
 10 -172.85 2.0  
 10 -173.43 2.0  
 10 -173.91 2.0  
 10 -174.49 2.0  
 10 -174.97 2.0  
 10 -175.55 2.0  
 10 -176.13 2.0  
 10 -176.71 2.0  
 10 -177.29 2.0  
 10 -177.87 2.0  
 10 -178.45 2.0  
 10 -178.93 2.0  
 10 -179.51 2.0  
 10 -180.09 2.0  
 10 -180.67 2.0  
 10 -181.25 2.0  
 10 -181.83 2.0  
 10 -182.41 2.0  
 10 -182.99 2.0  
 10 -183.57 2.0  
 10 -184.15 2.0  
 10 -184.73 2.0  
 10 -185.31 2.0  
 10 -185.89 2.0  
 10 -186.47 2.0  
 10 -187.05 2.0  
 10 -187.63 2.0  
 10 -188.21 2.0  
 10 -188.79 2.0  
 10 -189.37 2.0  
 10 -189.95 2.0  
 10 -190.53 2.0  
 10 -191.11 2.0  
 10 -191.69 2.0  
 10 -192.27 2.0  
 10 -192.85 2.0  
 10 -193.43 2.0  
 10 -193.91 2.0  
 10 -194.49 2.0  
 10 -194.97 2.0  
 10 -195.55 2.0  
 10 -196.13 2.0  
 10 -196.71 2.0  
 10 -197.29 2.0  
 10 -197.87 2.0  
 10 -198.45 2.0  
 10 -198.93 2.0  
 10 -199.51 2.0  
 10 -200.09 2.0  
 10 -200.67 2.0  
 10 -201.25 2.0  
 10 -201.83 2.0  
 10 -202.41 2.0  
 10 -202.99 2.0  
 10 -203.57 2.0  
 10 -204.15 2.0  
 10 -204.73 2.0  
 10 -205.31 2.0  
 10 -205.89 2.0  
 10 -206.47 2.0  
 10 -207.05 2.0  
 10 -207.63 2.0  
 10 -208.21 2.0  
 10 -208.79 2.0  
 10 -209.37 2.0  
 10 -209.95 2.0  
 10 -210.53 2.0  
 10 -211.11 2.0  
 10 -211.69 2.0  
 10 -212.27 2.0  
 10 -212.85 2.0  
 10 -213.43 2.0  
 10 -213.91 2.0  
 10 -214.49 2.0  
 10 -214.97 2.0  
 10 -215.55 2.0  
 10 -216.13 2.0  
 10 -216.71 2.0  
 10 -217.29 2.0  
 10 -217.87 2.0  
 10 -218.45 2.0  
 10 -218.93 2.0  
 10 -219.51 2.0  
 10 -220.09 2.0  
 10 -220.67 2.0  
 10 -221.25 2.0  
 10 -221.83 2.0  
 10 -222.41 2.0  
 10 -222.99 2.0  
 10 -223.57 2.0  
 10 -224.15 2.0  
 10 -224.73 2.0  
 10 -225.31 2.0  
 10 -225.89 2.0  
 10 -226.47 2.0  
 10 -227.05 2.0  
 10 -227.63 2.0  
 10 -228.21 2.0  
 10 -228.79 2.0  
 10 -229.37 2.0  
 10 -229.95 2.0  
 10 -230.53 2.0  
 10 -231.11 2.0  
 10 -231.69 2.0  
 10 -232.27 2.0  
 10 -232.85 2.0  
 10 -233.43 2.0  
 10 -233.91 2.0  
 10 -234.49 2.0  
 10 -234.97 2.0  
 10 -235.55 2.0  
 10 -236.13 2.0  
 10 -236.71 2.0  
 10 -237.29 2.0  
 10 -237.87 2.0  
 10 -238.45 2.0  
 10 -238.93 2.0  
 10 -239.51 2.0  
 10 -240.09 2.0  
 10 -240.67 2.0  
 10 -241.25 2.0  
 10 -241.83 2.0  
 10 -242.41 2.0  
 10 -242.99 2.0  
 10 -243.57 2.0  
 10 -244.15 2.0  
 10 -244.73 2.0  
 10 -245.31 2.0  
 10 -245.89 2.0  
 10 -246.47 2.0  
 10 -247.05 2.0  
 10 -247.63 2.0  
 10 -248.21 2.0  
 10 -248.79 2.0  
 10 -249.37 2.0  
 10 -249.95 2.0  
 10 -250.53 2.0  
 10 -251.11 2.0  
 10 -251.69 2.0  
 10 -252.27 2.0  
 10 -252.85 2.0  
 10 -253.43 2.0  
 10 -253.91 2.0  
 10 -254.49 2.0  
 10 -254.97 2.0  
 10 -255.55 2.0  
 10 -256.13 2.0  
 10 -256.71 2.0  
 10 -257.29 2.0  
 10 -257.87 2.0  
 10 -258.45 2.0  
 10 -258.93 2.0  
 10 -259.51 2.0  
 10 -260.09 2.0  
 10 -260.67 2.0  
 10 -261.25 2.0  
 10 -261.83 2.0  
 10 -262.41 2.0  
 10 -262.99 2.0  
 10 -263.57 2.0  
 10 -264.15 2.0  
 10 -264.73 2.0  
 10 -265.31 2.0  
 10 -265.89 2.0  
 10 -266.47 2.0  
 10 -267.05 2.0  
 10 -267.63 2.0  
 10 -268.21 2.0  
 10 -268.79 2.0  
 10 -269.37 2.0  
 10 -269.95 2.0  
 10 -270.53 2.0  
 10 -271.11 2.0  
 10 -271.69 2.0  
 10 -272.27 2.0  
 10 -272.85 2.0  
 10 -273.43 2.0  
 10 -273.91 2.0  
 10 -274.49 2.0  
 10 -274.97 2.0  
 10 -275.55 2.0  
 10 -276.13 2.0  
 10 -276.71 2.0  
 10 -277.29 2.0  
 10 -277.87 2.0  
 10 -278.45 2.0  
 10 -278.93 2.0  
 10 -279.51 2.0  
 10 -280.09 2.0  
 10 -280.67 2.0  
 10 -281.25 2.0  
 10 -281.83 2.0  
 10 -282.41 2.0  
 10 -282.99 2.0  
 10 -283.57 2.0  
 10 -284.15 2.0  
 10 -284.73 2.0  
 10 -285.31 2.0  
 10 -285.89 2.0  
 10 -286.47 2.0  
 10 -287.05 2.0  
 10 -287.63 2.0  
 10 -288.21 2.0  
 10 -288.79 2.0  
 10 -289.37 2.0  
 10 -289.95 2.0  
 10 -290.53 2.0  
 10 -291.11 2.0  
 10 -291.69 2.0  
 10 -292.27 2.0  
 10 -292.85 2.0  
 10 -293.43 2.0  
 10 -293.91 2.0  
 10 -294.49 2.0  
 10 -294.97 2.0  
 10 -295.55 2.0  
 10 -296.13 2.0  
 10 -296.71 2.0  
 10 -297.29 2.0  
 10 -297.87 2.0  
 10 -298.45 2.0  
 10 -298.93 2.0  
 10 -299.51 2.0  
 10 -300.09 2.0  
 10 -300.67 2.0  
 10 -301.25 2.0  
 10 -301.83 2.0  
 10 -302.41 2.0  
 10 -302.99 2.0  
 10 -303.57 2.0  
 10 -304.15 2.0  
 10 -304.73 2.0  
 10 -305.31 2.0  
 10 -305.89 2.0  
 10 -306.47 2.0  
 10 -307.05 2.0  
 10 -307.63 2.0  
 10 -308.21 2.0  
 10 -308.79 2.0  
 10 -309.37 2.0  
 10 -309.95 2.0  
 10 -310.53 2.0  
 10 -311.11 2.0  
 10 -311.69 2.0  
 10 -312.27 2.0  
 10 -312.85 2.0  
 10 -313.43 2.0  
 10 -313.91 2.0  
 10 -314.49 2.0  
 10 -314.97 2.0  
 10 -315.55 2.0  
 10 -316.13 2.0  
 10 -316.71 2.0  
 10 -317.29 2.0  
 10 -317.87 2.0  
 10 -318.45 2.0  
 10 -318.93 2.0  
 10 -319.51 2.0  
 10 -320.09 2.0  
 10 -320.67 2.0  
 10 -321.25 2.0  
 10 -321.83 2.0  
 10 -322.41 2.0  
 10 -322.99 2.0  
 10 -323.57 2.0  
 10 -324.15 2.0  
 10 -324.73 2.0  
 10 -325.31 2.0  
 10 -325.89 2.0  
 10 -326.47 2.0  
 10 -327.05 2.0  
 10 -327.63 2.0  
 10 -328.21 2.0  
 10 -328.79 2.0  
 10 -329.37 2.0  
 10 -329.95 2.0  
 10 -330.53 2.0  
 10 -331.11 2.0  
 10 -331.69 2.0  
 10 -332.27 2.0  
 10 -332.85 2.0  
 10 -333.43 2.0  
 10 -333.91 2.0  
 10 -334.49 2.0  
 10 -334.97 2.0  
 10 -335.55 2.0  
 10 -336.13 2.0  
 10 -336.71 2.0  
 10 -337.29 2.0  
 10 -337.87 2.0  
 10 -338.45 2.0  
 10 -338.93 2.0  
 10 -339.51 2.0  
 10 -340.09 2.0  
 10 -340.67 2.0  
 10 -341.25 2.0  
 10 -341.83 2.0  
 10 -342.41 2.0  
 10 -342.99 2.0  
 10 -343.57 2.0  
 10 -344.15 2.0  
 10 -344.73 2.0  
 10 -345.31 2.0  
 10 -345.89 2.0  
 10 -346.47 2.0  
 10 -347.05 2.0  
 10 -347.63 2.0  
 10 -348.21 2.0  
 10 -348.79 2.0  
 10 -349.37 2.0  
 10 -349.95 2.0  
 10 -350.53 2.0  
 10 -351.11 2.0  
 10 -351.69 2.0  
 10 -352.27 2.0  
 10 -352.85 2.0  
 10 -353.43 2.0  
 10 -353.91 2.0  
 10 -354.49 2.0  
 10 -354.97 2.0  
 10 -355.55 2.0  
 10 -356.13 2.0  
 10 -356.71 2.0  
 10 -357.29 2.0  
 10 -357.87 2.0  
 10 -358.45 2.0  
 10 -358.93 2.0  
 10 -359.51 2.0  
 10 -360.09 2.0  
 10 -360.67 2.0  
 10 -361.25 2.0  
 10 -361.83 2.0  
 10 -362.41 2.0  
 10 -362.99 2.0  
 10 -363.57 2.0  
 10 -364.15 2.0  
 10 -364.73 2.0  
 10 -365.31 2.0  
 10 -365.89 2.0  
 10 -366.47 2.0  
 10 -367.05 2.0  
 10 -367.63 2.0  
 10 -368.21 2.0  
 10 -368.79 2.0  
 10 -369.37 2.0  
 10 -369.95 2.0  
 10 -370.53 2.0  
 10 -371.11 2.0  
 10 -371.69 2.0  
 10 -372.27 2.0  
 10 -372.85 2.0  
 10 -373.43 2.0  
 10 -373.91 2.0  
 10 -374.49 2.0  
 10 -374.97 2.0  
 10 -375.55 2.0  
 10 -376.13 2.0  
 10 -376.71 2.0  
 10 -377.29 2.0  
 10 -377.87 2.0  
 10 -378.45 2.0  
 10 -378.93 2.0  
 10 -379.51 2.0  
 10 -380.09 2.0  
 10 -380.67 2.0  
 10 -381.25 2.0  
 10 -381.83 2.0  
 10 -382.41 2.0  
 10 -382.99 2.0  
 10 -383.57 2.0  
 10 -384.15 2.0  
 10 -384.73 2.0  
 10 -385.31 2.0  
 10 -385.89 2.0  
 10 -386.47 2.0  
 10 -387.05 2.0  
 10 -387.63 2.0  
 10 -388.21 2.0  
 10 -388.79 2.0  
 10 -389.37 2.0  
 10 -389.95 2.0  
 10 -390.53 2.0  
 10 -391.11 2.0  
 10 -391.69 2.0  
 10 -392.27 2.0  
 10 -392.85 2.0  
 10 -393.43 2.0  
 10 -393.91 2.0  
 10 -394.49 2.0  
 10 -394.97 2.0  
 10 -395.55 2.0  
 10 -396.13 2.0  
 10 -396.71 2.0  
 10 -397.29 2.0  
 10 -397.87 2.0  
 10 -398.45 2.0  
 10 -398.93 2.0  
 10 -399.51 2.0  
 10 -400.09 2.0  
 10 -400.67 2.0  
 10 -401.25 2.0  
 10 -401.83 2.0  
 10 -402.41 2.0  
 10 -

$$EIN = 0.16666 \cdot 0.154 = 0.02566$$

EIN = EINSTEIN

```

10 7321 1E+00
10 434201E+00
10 341931E+00
10 154395E+00
10 75451E+00
10 425604E+00
10 241861E+00
10 137441E+00
10 780560E+00
10 442530E+00
10 248423E+00
10 140536E+00
10 745361E+00
21 10 461413E+00
22 10 184447E+00
23 10 565213E+00
24 10 753822E+00
35 0.534360E+00
SUM OF (L+1)*X(L+1) = 2.09587E+01
TOTAL SUM = 0.415510E+01
BETHE APPROXIMATION = 0.43187E+01
OF ABE = 0.213230E+01

```

LIN = 0 EQUATION 400

```

10 8873032E+00
10 16235378E+00
10 6142792E+00
10 289524E+00
10 173673E+00
10 103535E+00
10 711937E+00
10 476677E+00
10 226336E+00
10 158693E+00
10 111323E+00
10 795503E+00
10 571482E+00
10 413613E+00
10 290323E+00
10 161223E+00
10 109557E+00
10 111363E+00
10 86242E+00
10 634372E+00
10 434393E+00
10 344521E+00
10 258779E+00
10 190630E+00
10 124737E+00
10 851127E+00
10 636325E+00
10 465486E+00
10 307005E+00
10 182173E+00
10 114100E+00
10 750455E+00
10 590295E+00
10 460511E+00
10 341272E+00

```

LINE = 1 EQUATION 401

COEFFICIENTS OF X(L)

LINE = 2 EQUATION 402

SUM OF  $\langle L+1 \rangle \times C_{L+1}^L$  = 0.4636E+01  
TOTAL SUM = 0.250000E+02  
BETHE APPROXIMATION = 0.971725E+05  
DF/CE = 0.166715E+01

EIN = C 149343E+02

1.000000E+00  
-0.162613E+01  
-0.162613E+01  
-0.433613E+00  
-0.350143E+00  
-0.218763E+00  
-0.151693E+00  
-0.110553E+00  
-0.831013E-01  
-0.637523E-01  
-0.493533E-01  
-0.369213E-01  
-0.303433E-01  
-0.245373E-01  
-0.198144E-01  
-0.160323E-01  
-0.130414E-01  
-0.105571E-01  
-0.874353E-02  
-0.719646E-02  
-0.594416E-02  
-0.452123E-02  
-0.408367E-02  
-0.339513E-02  
-0.282732E-02  
-0.235691E-02  
-0.197037E-02  
-0.164749E-02  
-0.137949E-02  
-0.115650E-02  
-0.967674E-02  
-0.813013E-02  
-0.683581E-02  
-0.574657E-02  
-0.483536E-02  
-0.407643E-02  
-0.342846E-02  
-0.266800E-02  
-0.243564E-02  
-0.205459E-02  
SUM OF  $\langle L+1 \rangle \times C_{L+1}^L$  = 0.250000E+02  
TOTAL SUM = 0.250000E+02  
BETHE APPROXIMATION = 0.971725E+05  
DF/CE = 0.149343E+01

EIN = 0.250000E+02

ANALYSIS = 0.971725E+05  
TEST = 1.49343E+01

**Copy available to ERIC does not  
permit fully legible reproduction**

```

-0. 5746 1.0E-01
-0. 753.61.0E-01
-0. 453537E-01
-0. 572674E-01
-0. 575132E-01
-0. 42794.0E-01
-0. 359289E-01
-0. 35721.1E-01
-0. 320593E-01
-0. 283263E-01
-0. 26171.7E-01
-0. 22374.1E-01
-0. 21595.0E-01
-0. 19693.2E-01
-0. 17754.3E-01
-0. 16473.3E-01
-0. 15119.2E-01
-0. 1239.6E-01
-0. 12752.6E-01
-0. 11783.6E-01
-0. 1055.9E-01
-0. 10451.6E-01
-0. 925.537E-01
-0. 857.21.0E-01
-0. 7955.43E-01
-0. 732.61.0E-01
-0. 684.036E-01
-0. 6254.42E-01
-0. 5502.55E-01
-0. 54851.1E-01
SUM OF C1+10**X1+C11*X2 = 0. 753438E-01
TOTAL SUM = 0. 135517E-01
BETWEEN APPROPRIATE Z = 0. 176506E-01
DEGREE = 0

```

EIN =	C. SYNTHETIC	C2	CHEM	G	UNIVERSAL
L	$\delta(\text{LL}+1)$	$\delta(\text{L}+1)$	$\delta(\text{L}+1)$	$\delta(\text{L}+1)$	$\delta(\text{L}+1)$
0	$-C \cdot 157.37E+01$	$C \cdot 0.000000E+00$	$C \cdot 0.000000E+00$	$C \cdot 0.000000E+00$	$C \cdot 0.000000E+00$
1	$-0 \cdot 1038.78E-4.01$	$-0 \cdot 1.3630E-4.01$	$-0 \cdot 1.3630E-4.01$	$-0 \cdot 1.3630E-4.01$	$-0 \cdot 1.3630E-4.01$
2	$-0 \cdot 4567.1CE+01$	$-0 \cdot 9845.34E+00$	$-0 \cdot 9845.34E+00$	$-0 \cdot 9845.34E+00$	$-0 \cdot 9845.34E+00$
3	$-0 \cdot 4339.17E+01$	$-0 \cdot 1851.01E+01$	$-0 \cdot 1851.01E+01$	$-0 \cdot 1851.01E+01$	$-0 \cdot 1851.01E+01$
4	$-0 \cdot 3087.9E+00$	$-0 \cdot 2585.72E+00$	$-0 \cdot 2585.72E+00$	$-0 \cdot 2585.72E+00$	$-0 \cdot 2585.72E+00$
5	$-0 \cdot 2271.24E+00$	$-0 \cdot 2616.24E+00$	$-0 \cdot 2616.24E+00$	$-0 \cdot 2616.24E+00$	$-0 \cdot 2616.24E+00$
6	$-0 \cdot 1745.7CE+00$	$-0 \cdot 1370.33E+00$	$-0 \cdot 1370.33E+00$	$-0 \cdot 1370.33E+00$	$-0 \cdot 1370.33E+00$
7	$-0 \cdot 1393.19E+00$	$-0 \cdot 7232.42E-01$	$-0 \cdot 7232.42E-01$	$-0 \cdot 7232.42E-01$	$-0 \cdot 7232.42E-01$
8	$-0 \cdot 1156.76E+00$	$-0 \cdot 7251.69E-01$	$-0 \cdot 7251.69E-01$	$-0 \cdot 7251.69E-01$	$-0 \cdot 7251.69E-01$
9	$-0 \cdot 7824.72E-01$	$-0 \cdot 5756.34E-01$	$-0 \cdot 5756.34E-01$	$-0 \cdot 5756.34E-01$	$-0 \cdot 5756.34E-01$
10	$-0 \cdot 6513.55E-01$	$-0 \cdot 4446.23E-01$	$-0 \cdot 4446.23E-01$	$-0 \cdot 4446.23E-01$	$-0 \cdot 4446.23E-01$
11	$-0 \cdot 7489.02E-01$	$-0 \cdot 3641.34E-01$	$-0 \cdot 3641.34E-01$	$-0 \cdot 3641.34E-01$	$-0 \cdot 3641.34E-01$
12	$-0 \cdot 4462.02E-01$	$-0 \cdot 3675.35E-01$	$-0 \cdot 3675.35E-01$	$-0 \cdot 3675.35E-01$	$-0 \cdot 3675.35E-01$
13	$-0 \cdot 5978.14E-01$	$-0 \cdot 2579.17E-01$	$-0 \cdot 2579.17E-01$	$-0 \cdot 2579.17E-01$	$-0 \cdot 2579.17E-01$
14	$-0 \cdot 5406.01E-01$	$-0 \cdot 2177.66E-01$	$-0 \cdot 2177.66E-01$	$-0 \cdot 2177.66E-01$	$-0 \cdot 2177.66E-01$
15	$-0 \cdot 4904.04E-01$	$-0 \cdot 1871.34E-01$	$-0 \cdot 1871.34E-01$	$-0 \cdot 1871.34E-01$	$-0 \cdot 1871.34E-01$
16	$-0 \cdot 4473.61E-01$	$-0 \cdot 1624.99E-01$	$-0 \cdot 1624.99E-01$	$-0 \cdot 1624.99E-01$	$-0 \cdot 1624.99E-01$
17	$-0 \cdot 4036.9E-01$	$-0 \cdot 1418.86E-01$	$-0 \cdot 1418.86E-01$	$-0 \cdot 1418.86E-01$	$-0 \cdot 1418.86E-01$
18	$-0 \cdot 3546.72E-01$	$-0 \cdot 1213.61E-01$	$-0 \cdot 1213.61E-01$	$-0 \cdot 1213.61E-01$	$-0 \cdot 1213.61E-01$

**Copy available on microfilm only**

卷之三

卷之三

23 -0. 561203E-01 -0. 399261E-06  
 24 -0. 344543E-01 -0. 324265E-06  
 25 -0. 269135E-05 -0. 214661E-06  
 26 -0. 111443E-05 -0. 125123E-06  
 27 -0. 537373E-04 -0. 628962E-06  
 28 -0. 281841E-04 -0. 299575E-06  
 29 -0. 774573E-04 -0. 454575E-06  
 30 -0. 782602E-07 -0. 651037E-07  
 SUM OF (L+1)\*X(L+1)\*X(L+1) = 0. 7185512E+01  
 TOTAL SUM = 0. 7185512E+01  
 BETHE APPROXIMATION = 0. 7409710E+01  
 DF/DE = 0. 249121E+00

EIN = 0. 100000E+02

L X(L+1) X(L+1) X(L+1) X(L+1)

0 -0. 127251E+01 0. 000000E+00 0. 151726E+01 0. 000000E+00  
 1 -0. 124253E+01 0. 455453E+00 0. 150713E+01 0. 455453E+00  
 2 -0. 7CB7B5E+09 0. 265236E+00 0. 150713E+01 0. 455453E+00  
 3 -0. 2492293E+00 0. 570573E+01 0. 150713E+01 0. 455453E+00  
 4 -0. 152664E+00 0. 551401E+01 0. 150713E+01 0. 455453E+00  
 5 -0. 117423E+00 0. 156152E+01 0. 150713E+01 0. 455453E+00  
 6 -0. 750515E+01 0. 167235E+01 0. 150713E+01 0. 455453E+00  
 7 -0. 507923E+01 0. 553277E+01 0. 150713E+01 0. 455453E+00  
 8 -0. 348542E+01 0. 417233E+01 0. 150713E+01 0. 455453E+00  
 9 -0. 241678E+01 0. 254664E+01 0. 150713E+01 0. 455453E+00  
 10 -0. 165721E+01 0. 174177E+01 0. 150713E+01 0. 455453E+00  
 11 -0. 112836E+01 0. 115633E+01 0. 150713E+01 0. 455453E+00  
 12 -0. 841655E+01 0. 743746E+01 0. 150713E+01 0. 455453E+00  
 13 -0. 593944E+01 0. 429273E+01 0. 150713E+01 0. 455453E+00  
 14 -0. 429273E+01 0. 307232E+01 0. 150713E+01 0. 455453E+00  
 15 -0. 307232E+01 0. 242321E+01 0. 150713E+01 0. 455453E+00  
 16 -0. 221763E+01 0. 165192E+01 0. 150713E+01 0. 455453E+00  
 17 -0. 1604735E+01 0. 1153772E+01 0. 150713E+01 0. 455453E+00  
 18 -0. 115344E+01 0. 846642E+01 0. 150713E+01 0. 455453E+00  
 19 -0. 846642E+01 0. 620124E+01 0. 150713E+01 0. 455453E+00  
 20 -0. 620124E+01 0. 454775E+01 0. 150713E+01 0. 455453E+00  
 21 -0. 454775E+01 0. 333724E+01 0. 150713E+01 0. 455453E+00  
 22 -0. 333724E+01 0. 232365E+01 0. 150713E+01 0. 455453E+00  
 23 -0. 245359E+01 0. 155812E+01 0. 150713E+01 0. 455453E+00  
 24 -0. 185823E+01 0. 107752E+01 0. 150713E+01 0. 455453E+00  
 25 -0. 133517E+01 0. 7246772E+00 0. 150713E+01 0. 455453E+00  
 26 -0. 966776E+01 0. 4737793E+01 0. 150713E+01 0. 455453E+00  
 27 -0. 734229E+01 0. 326211E+01 0. 150713E+01 0. 455453E+00  
 28 -0. 544574E+01 0. 245223E+01 0. 150713E+01 0. 455453E+00  
 29 -0. 404520E+01 0. 162827E+01 0. 150713E+01 0. 455453E+00  
 30 -0. 302114E+01 0. 105233E+01 0. 150713E+01 0. 455453E+00  
 31 -0. 226164E+01 0. 721438E+01 0. 150713E+01 0. 455453E+00  
 32 -0. 165587E+01 0. 536332E+01 0. 150713E+01 0. 455453E+00  
 33 -0. 12519CE+01 0. 363729E+01 0. 150713E+01 0. 455453E+00  
 34 -0. 931643E+01 0. 275254E+01 0. 150713E+01 0. 455453E+00  
 35 -0. 697578E+01 0. 131543E+01 0. 150713E+01 0. 455453E+00  
 36 -0. 528272E+01 0. 517245E+01 0. 150713E+01 0. 455453E+00  
 37 -0. 402989E+01 0. 581640E+01 0. 150713E+01 0. 455453E+00  
 38 -0. 304368E+01 0. 107859E+01 0. 150713E+01 0. 455453E+00  
 SUM OF (L+1)\*X(L+1)\*X(L+1) = 0. 6227710E+01  
 TOTAL SUM = 0. 6227710E+01



$\begin{aligned}
& -0.116039E+01 \\
& -0.725794E+01 \\
& -0.452743E+01 \\
& -0.275294E+01 \\
& -0.151354E+01 \\
& -0.115213E+01 \\
& -0.915841E+01 \\
& -0.741767E+01 \\
& -0.568273E+01 \\
& -0.504063E+01 \\
& -0.420953E+01 \\
& -0.357611E+01 \\
& -0.298422E+01 \\
& -0.252844E+01 \\
& -0.214971E+01 \\
& -0.183343E+01 \\
& -0.156803E+01 \\
& -0.124509E+01 \\
& -0.115541E+01 \\
& -0.98715E+00 \\
& -0.860541E+00 \\
& -0.745204E+00 \\
& -0.646277E+00 \\
& -0.561279E+00 \\
& -0.485622E+00 \\
& -0.425813E+00 \\
& -0.371391E+00 \\
& -0.324917E+00 \\
& -0.284349E+00 \\
& -0.242111E+00 \\
& -0.218477E+00 \\
& -0.191803E+00 \\
& -0.168530E+00 \\
& -0.142201E+00 \\
& -0.130433E+00 \\
& -0.114846E+00 \\
& -0.101203E+00
\end{aligned}$

$\begin{aligned}
& +0.117320E+01 \\
& +0.663632E+01 \\
& +0.364337E+01 \\
& +0.204673E+01 \\
& +0.115452E+01 \\
& +0.731325E+01 \\
& +0.472221E+01 \\
& +0.321403E+01 \\
& +0.229451E+01 \\
& +0.169572E+01 \\
& +0.128403E+01 \\
& +0.950214E+01 \\
& +0.755614E+01 \\
& +0.605949E+01 \\
& +0.465743E+01 \\
& +0.346111E+01 \\
& +0.246202E+01 \\
& +0.175157E+01 \\
& +0.125715E+01 \\
& +0.855671E+01 \\
& +0.646949E+01 \\
& +0.469749E+01 \\
& +0.330635E+01 \\
& +0.247823E+01 \\
& +0.182640E+01 \\
& +0.137949E+01 \\
& +0.985410E+01 \\
& +0.705574E+01 \\
& +0.492274E+01 \\
& +0.352624E+01 \\
& +0.231794E+01 \\
& +0.177951E+01 \\
& +0.134649E+01 \\
& +0.914645E+01 \\
& +0.671625E+01 \\
& +0.457274E+01 \\
& +0.326340E+01 \\
& +0.206433E+01 \\
& +0.156419E+01 \\
& +0.115406E+01 \\
& +0.814053E+01 \\
& +0.585326E+01 \\
& +0.406751E+01 \\
& +0.287274E+01 \\
& +0.195617E+01 \\
& +0.147545E+01 \\
& +0.103136E+01 \\
& +0.757545E+01 \\
& +0.527724E+01 \\
& +0.360751E+01 \\
& +0.246174E+01 \\
& +0.172736E+01 \\
& +0.124739E+01 \\
& +0.863528E+01 \\
& +0.605634E+01 \\
& +0.406433E+01 \\
& +0.273491E+01 \\
& +0.195617E+01 \\
& +0.142027E+01 \\
& +0.101215E+01 \\
& +0.761733E+01 \\
& +0.517454E+01 \\
& +0.354954E+01 \\
& +0.231793E+01 \\
& +0.167723E+01 \\
& +0.122609E+01 \\
& +0.876526E+01 \\
& +0.626526E+01 \\
& +0.436247E+01 \\
& +0.303214E+01 \\
& +0.207561E+01 \\
& +0.157521E+01 \\
& +0.112515E+01 \\
& +0.787526E+01 \\
& +0.542921E+01 \\
& +0.375427E+01 \\
& +0.250753E+01 \\
& +0.187973E+01
\end{aligned}$

$$\begin{aligned}
& \text{TOTAL SUM = } 0.115479E+02 \\
& \text{BETHE APPROXIMATION = } 0.124764E+02 \\
& \text{DF/CE = } 0.176594E+00
\end{aligned}$$

$$EIN = 0.5 * LOG(CE/CE)$$

$$L = \sqrt{1 + 1/L^2}$$

$\begin{aligned}
& 0.167442E+01 \\
& -0.113535E+01 \\
& -0.717179E+01 \\
& -0.477603E+01 \\
& -0.320121E+01 \\
& -0.260903E+01 \\
& -0.181363E+01 \\
& -0.147723E+01 \\
& -0.117005E+01 \\
& -0.952517E+01 \\
& -0.393353E+01
\end{aligned}$

$\begin{aligned}
& 0.223772E+01 \\
& 0.156777E+01 \\
& 0.155145E+01 \\
& 0.112324E+01 \\
& 0.114757E+01 \\
& 0.104343E+01 \\
& 0.951853E+01 \\
& 0.875424E+01 \\
& 0.807514E+01 \\
& 0.747773E+01 \\
& 0.696773E+01 \\
& 0.654773E+01 \\
& 0.619773E+01 \\
& 0.589773E+01 \\
& 0.562773E+01 \\
& 0.536773E+01 \\
& 0.512773E+01 \\
& 0.490773E+01 \\
& 0.470773E+01 \\
& 0.452773E+01 \\
& 0.436773E+01 \\
& 0.422773E+01 \\
& 0.410773E+01 \\
& 0.400773E+01
\end{aligned}$

Copy available at GNGC does not  
permit fully legible reproduction

$E_1 = -0.667374E-01$   
 $-0.594442E-01$   
 $-0.518294E-01$   
 $14 -0.454689E-01$   
 $-0.400833E-01$   
 $-0.354761E-01$   
 $-0.315620E-01$   
 $15 -0.280552E-01$   
 $-0.250494E-01$   
 $-0.224163E-01$   
 $-0.201030E-01$   
 $16 -0.180304E-01$   
 $-0.152717E-01$   
 $-0.145734E-01$   
 $-0.132655E-01$   
 $17 -0.120042E-01$   
 $-0.105811E-01$   
 $-0.987621E-01$   
 $18 -0.912034E-01$   
 $-0.837623E-01$   
 $-0.767743E-01$   
 $19 -0.704761E-01$   
 $-0.644633E-01$   
 $20 -0.592063E-01$   
 $-0.546352E-01$   
 $-0.497732E-01$   
 $21 -0.457131E-01$   
 $-0.417135E-01$   
 $-0.376235E-01$   
 $22 -0.336232E-01$   
 $-0.297131E-01$   
 $-0.260686E-01$   
 $23 -0.221135E-01$   
 $-0.187135E-01$   
 $-0.155911E-01$   
 $24 -0.127232E-01$   
 $-0.104336E-01$   
 $-0.860936E-01$   
 $25 -0.712361E-01$   
 $-0.518477E-01$   
 $-0.424743E-01$   
 $26 -0.435020E-01$   
 $-0.398932E-01$   
 $TOTAL SUM = 0.136017E+02$   
 $BETHE APPROXIMATION = 0$   
 $DF/DE = 0.163486E+00$   
 $STEP STEP1$   
 $C. 500000E+02 0.000000E+00$   
 $SUM OF (L+1)*X(L+1)*E(L+1)$   
 $TOTAL SUM = 0.140000E+02$   
 $BETHE APPROXIMATION = 0$

$EIN = C. 1000000E+01$

$L$

$0$	$-0.154763E+01$	$0.000000E+00$	$0.233273E+01$
$1$	$-0.165262E+01$	$-0.530112E+00$	$0.543116E+01$
$2$	$-0.467950E+01$	$-0.162632E+00$	$0.624550E+00$
$3$	$-0.722523E+01$	$-0.265000E+01$	$0.312577E+01$
$4$	$0.134463E+01$	$-0.364610E+02$	$0.931324E+01$
$5$	$-0.283930E+01$	$-0.563111E+02$	$0.483779E+01$
$6$	$-0.632545E+01$	$-0.861704E+02$	$0.280179E+01$
$7$	$0.146700E+01$	$-0.152811E+02$	$0.174116E+01$
$8$	$-0.349793E+01$	$-0.267345E+02$	$0.110351E+01$
$9$	$-0.834637E+01$	$-0.511672E+02$	$0.467611E+01$
$10$	$-0.202172E+01$	$-0.465924E+02$	$0.349534E+01$
$11$	$-0.725912E+01$	$-0.282026E+02$	$0.244979E+01$
$12$	$-0.364502E+01$	$0.143674E+02$	$0.151265E+01$
$13$	$-0.114634E+01$	$-0.420424E+02$	$0.182722E+01$
$14$	$-0.461372E+01$	$-0.296831E+02$	$0.146454E+01$
$15$	$0.323053E+01$	$-0.465661E+02$	$0.104739E+01$

SUM OF (L+1)\*X(L+1)\*E(L+1) = 0.000041E+01

TOTAL SUM = 0.3746161F+01

BETHE APPROXIMATION = 0.373871E+01



EIN = 0, 1000000F, 02		CIF(0) = 0, 1438360E+00		CIF(1) = 0, 1438360E+00		CIF(2) = 0, 1438360E+00	
L	X(L+1)	0	164938E+01	0	303600E+00	0	272214E+00
0	-0	145446E+01	-0	799853E+00	0	467534E+01	0
1	-0	732747E+00	-0	354576E+00	0	161074E+01	0
2	-0	364463E+00	-0	132363E+00	0	376866E+00	0
3	-0	130433E+00	-0	521552E+01	0	956172E+01	0
4	-0	66977CE-01	-0	202374E-01	0	265677E-01	0
5	-0	346778E-01	-0	821811E-02	0	241283E-02	0
6	-0	263604E-01	-0	354251E-02	0	32297CE-02	0
7	-0	116567E-01	-0	163468E-02	0	12269CE-02	0
8	-0	473537E-02	-0	605758E-03	0	461568E-03	0
9	-0	400864E-02	-0	421561E-03	0	175761E-03	0
0	-0	236451E-03	-0	250020E-03	0	68220CE-04	0
1	-0	142473E-03	-0	187328E-03	0	234430E-04	0
2	-0	554538E-03	-0	94070CE-04	0	167913E-04	0
3	-0	51587CE-03	-0	427652E-04	0	354793E-04	0
4	-0	311030E-03	-0	967656E-04	0	102365E-03	0
5	-0	188445E-03	-0	145528E-04	0	487823E-04	0
6	-0	114253E-03	-0	636505E-05	0	233756E-04	0
7	-0	694413E-03	-0	3797415E-05	0	914727E-03	0
8	-0	421143E-03	-0	195855E-05	0	3754727L-03	0
9	-0	255874E-03	-0	103657E-05	0	123032E-03	0
0	-0	156403E-03	-0	511357E-05	0	673645E-03	0
1	-0	724472E-03	-0	27450E-05	0	324301E-03	0
2	-0	524575E-02	-0	179232E-05	0	1379717E-03	0
3	-0	350504E-02	-0	103424E-05	0	746724E-03	0
4	-0	206663E-01	-0	622967E-06	0	441646E-03	0
5	-0	123081E-01	-0	145636E-06	0	403683E-03	0
6	-0	750178E-01	-0	506357E-07	0	174352E-03	0
7	-0	464682E-01	-0	141945E-07	0	431266E-03	0
8	-0	157534E-01	-0	170565E-07	0	928136E-03	0
9	-0	578292E-01	-0	727241E-07	0	182377E-03	0
0	-0	162911E-01	-0	419632E-07	0	146377E-03	0
1	-0	465370E-01	-0	219211E-07	0	1000000E-03	0

33 0. 925611E-07 -0. 253753E-06 0. 951631E-12  
 34 0. 220702E-06 -0. 346479E-06 0. 170362E-11  
 35 0. 213564E-06 -0. 507555E-06 0. 144539E-11  
 36 0. 125836E-06 -0. 137277E-07 0. 682793E-11  
 37 0. 926684E-07 -0. 213512E-07 0. 525599E-11  
 38 0. 555532E-07 -0. 263039E-07 0. 120362E-11  
 SUM OF (L+1)\*XL(L+1) = 0. 925611E+01  
 TOTAL SUM = 0. 102182E+02  
 BETHE APPROXIMATION = 0. 749721E+00  
 DF/DE = C. 338307E-01

LIN = C. 2000000402

CHMGA = 0. 1450000402

X(L+1) = 0. 1450000402

LIN = 0. 1450000402

-0. 173297E+01 0. 000000E+00 0. 000000E+00  
 -0. 132753E+01 -0. 750. 00E+00 0. 303000E+00  
 -0. 787784E+00 -0. 475675E+00 0. 165164E+01  
 -0. 416877E+00 -0. 289632E+00 0. 595675E+00  
 -0. 231503E+00 -0. 164981E+00 0. 247967E+00  
 -0. 127204E+00 -0. 101310E+00 0. 147125E+00  
 -0. 858355E+01 -0. 660432E+01 0. 147125E+01  
 -0. 562375E+01 -0. 436775E+01 0. 147125E+01  
 -0. 377474E+01 -0. 252795E+01 0. 147125E+01  
 -0. 261630E+01 -0. 174025E+01 0. 147125E+01  
 -0. 163195E+01 -0. 117431E+01 0. 147125E+01  
 -0. 122502E+01 -0. 845772E+01 0. 147125E+01  
 -0. 922420E+01 -0. 614110E+01 0. 147125E+01  
 -0. 660213E+01 -0. 418165E+01 0. 147125E+01  
 -0. 474618E+01 -0. 287935E+01 0. 147125E+01  
 -0. 342105E+01 -0. 202795E+01 0. 147125E+01  
 -0. 247153E+00 -0. 148577E+00 0. 147125E+01  
 -0. 179000E+00 -0. 104110E+00 0. 147125E+01  
 -0. 129855E+00 -0. 712165E+00 0. 147125E+01  
 -0. 743872E+00 -0. 462055E+00 0. 147125E+01  
 -0. 465717E+00 -0. 289542E+00 0. 147125E+01  
 -0. 301065E+00 -0. 182842E+00 0. 147125E+01  
 -0. 348657E+00 -0. 127514E+00 0. 147125E+01  
 -0. 262702E+00 -0. 829213E+00 0. 147125E+01  
 -0. 196670E+00 -0. 547132E+00 0. 147125E+01  
 -0. 142873E+00 -0. 322238E+00 0. 147125E+01  
 -0. 105559E+00 -0. 193677E+00 0. 147125E+01  
 -0. 776374E+00 -0. 128602E+00 0. 147125E+01  
 -0. 572305E+00 -0. 103398E+00 0. 147125E+01  
 -0. 425177E+00 -0. 767314E+00 0. 147125E+01  
 -0. 421279E+00 -0. 267638E+00 0. 147125E+01  
 -0. 310651E+00 -0. 150367E+00 0. 147125E+01  
 -0. 223741E+00 -0. 102862E+00 0. 147125E+01  
 -0. 167255E+00 -0. 103398E+00 0. 147125E+01  
 -0. 125177E+00 -0. 722619E+00 0. 147125E+01  
 -0. 932955E+00 -0. 529736E+00 0. 147125E+01  
 -0. 684264E+00 -0. 301360E+00 0. 147125E+01  
 -0. 455778E+00 -0. 256592E+00 0. 147125E+01  
 -0. 369549E+00 -0. 192054E+00 0. 147125E+01  
 SUM OF (L+1)\*XL(L+1) = 0. 9929999999999999  
 TOTAL SUM = C. 114279E+02  
 BETHE APPROXIMATION = 0. 791323E+01  
 DF/DE = C. 349110E+01

36 -0. 276167E+00 -0. 141446E+00 0. 271323E+01  
 SUM OF (L+1)\*XL(L+1) = 0. 9929999999999999  
 TOTAL SUM = C. 114279E+02  
 BETHE APPROXIMATION = 0. 791323E+01  
 DF/DE = C. 349110E+01

EIN = C 320000E+02

CMEBA = C 146600E+02

X(L+1) = (L+1)\*X(L+1)\*\*2

L\*X(L+1)\*\*2

L  
0 -0.179450E+01 0.000000E+00 0.000000E+00 0.000000E+00  
1 -0.132814E+01 0.167050E+01 0.167050E+01 0.167050E+01  
2 -0.442716E+01 0.274214E+02 0.274214E+02 0.274214E+02  
3 -0.265619E+02 0.147177E+03 0.147177E+03 0.147177E+03  
4 -0.184075E+02 0.913500E+03 0.913500E+03 0.913500E+03  
5 -0.121746E+02 0.454680E+04 0.454680E+04 0.454680E+04  
6 -0.864864E+01 0.254260E+04 0.254260E+04 0.254260E+04  
7 -0.623533E+01 0.160923E+04 0.160923E+04 0.160923E+04  
8 -0.460278E+01 0.105632E+04 0.105632E+04 0.105632E+04  
9 -0.345510E+01 0.45732E+04 0.45732E+04 0.45732E+04  
10 -0.262378E+01 0.465670E+04 0.465670E+04 0.465670E+04  
11 -0.201114E+01 0.311550E+04 0.311550E+04 0.311550E+04  
12 -0.155141E+01 0.252460E+04 0.252460E+04 0.252460E+04  
13 -0.126279E+01 0.162929E+04 0.162929E+04 0.162929E+04  
14 -0.102521E+01 0.120505E+04 0.120505E+04 0.120505E+04  
15 -0.729455E+00 0.879416E+03 0.879416E+03 0.879416E+03  
16 -0.570810E+00 0.675935E+03 0.675935E+03 0.675935E+03  
17 -0.445370E+00 0.519243E+03 0.519243E+03 0.519243E+03  
18 -0.350624E+00 0.364771E+03 0.364771E+03 0.364771E+03  
19 -0.275635E+00 0.252765E+03 0.252765E+03 0.252765E+03  
20 -0.217019E+00 0.202561E+03 0.202561E+03 0.202561E+03  
21 -0.171133E+00 0.159193E+03 0.159193E+03 0.159193E+03  
22 -0.135432E+00 0.123869E+03 0.123869E+03 0.123869E+03  
23 -0.105862E+00 0.951215E+02 0.951215E+02 0.951215E+02  
24 -0.844184E+00 0.743710E+02 0.743710E+02 0.743710E+02  
25 -0.670673E+00 0.571692E+02 0.571692E+02 0.571692E+02  
26 -0.532624E+00 0.436517E+02 0.436517E+02 0.436517E+02  
27 -0.423297E+00 0.334574E+02 0.334574E+02 0.334574E+02  
28 -0.336803E+00 0.255681E+02 0.255681E+02 0.255681E+02  
29 -0.265313E+00 0.195664E+02 0.195664E+02 0.195664E+02  
30 -0.212221E+00 0.150947E+02 0.150947E+02 0.150947E+02  
31 -0.170617E+00 0.117447E+02 0.117447E+02 0.117447E+02  
32 -0.136524E+00 0.873534E+01 0.873534E+01 0.873534E+01  
33 -0.107912E+00 0.657776E+01 0.657776E+01 0.657776E+01  
34 -0.874234E+00 0.511095E+01 0.511095E+01 0.511095E+01  
35 -0.701611E+00 0.397566E+01 0.397566E+01 0.397566E+01  
36 -0.561264E+00 0.302193E+01 0.302193E+01 0.302193E+01  
37 -0.450273E+00 0.226221E+01 0.226221E+01 0.226221E+01  
38 -0.350000E+00 0.164927E+02 0.164927E+02 0.164927E+02  
SUM OF (L+1)\*X(L+1)\*\*2 = 0.1115170E+01  
TOTAL SUM = C.126132E+02  
BETHE APPROXIMATION = 0.1115170E+01  
DE/DCE = 0.241105E-01

OMEGA = 0.148000E+02

SUM OF (L+1)\*X(L+1)\*\*2 = 0.1115170E+01

BETHE APPROXIMATION = 0.1115170E+01

DE/DCE = 0.241105E-01

L\*X(L+1)\*\*2  
0.353474E+01 0.000000E+00  
0.326374E+01 0.156242E+01  
0.107674E+01 0.855031E+00

Copy available to FWC does not  
permit fully legible reproduction

**SAMPLE COMPUTER OUTPUT**

STEP STEP1  
0.310000E-02 0.500000E-03 0.130000E+02

USING THE DFT/INPUT POTENTIAL

Ne-like Al ion in Al plasma  
 $n = 2.2E+23$  T= 50 ev  
Bound-Free cross-sections  
from 1S-level

0.000000E+00	0.130001E+02
0.310000E-02	0.129925E+02
0.620000E-02	0.129839E+02
0.930000E-02	0.129743E+02
0.124000E-01	0.129636E+02
0.155000E-01	0.129521E+02
0.186000E-01	0.129398E+02
0.217000E-01	0.129267E+02
0.248000E-01	0.129128E+02
0.279000E-01	0.128983E+02
0.310000E-01	0.128831E+02
0.341000E-01	0.128673E+02
0.372000E-01	0.128510E+02
0.403000E-01	0.128341E+02
0.434000E-01	0.128168E+02
0.465000E-01	0.127990E+02
0.496000E-01	0.127808E+02
0.527000E-01	0.127622E+02
0.558000E-01	0.127433E+02
0.589000E-01	0.127240E+02

N= 1 L= 0

ALPHA = -0.77000000E+02	
LAST ZERO POINT I = 261	ZR = 0.28
ALPHA = -0.77099998E+02	
LAST ZERO POINT I = 261	ZR = 0.28
ALPHA = -0.77199997E+02	
LAST ZERO POINT I = 261	ZR = 0.28
ALPHA = -0.77299995E+02	
LAST ZERO POINT I = 271	ZR = 0.33
ALPHA = -0.77399994E+02	
LAST ZERO POINT I = 271	ZR = 0.33
ALPHA = -0.77499992E+02	
LAST ZERO POINT I = 271	ZR = 0.33
ALPHA = -0.77599991E+02	
LAST ZERO POINT I = 271	ZR = 0.33
ALPHA = -0.77699989E+02	
LAST ZERO POINT I = 271	ZR = 0.33
ALPHA = -0.77799988E+02	
LAST ZERO POINT I = 271	ZR = 0.33
ALPHA = -0.77899986E+02	
LAST ZERO POINT I = 271	ZR = 0.33

ALPHA = -0.77999985E+02	ZR = 0.33
LAST ZERO POINT I = 271	
ALPHA = -0.78099983E+02	ZR = 0.33
LAST ZERO POINT I = 271	
ALPHA = -0.78199982E+02	ZR = 0.33
LAST ZERO POINT I = 271	
ALPHA = -0.78299980E+02	ZR = 0.33
LAST ZERO POINT I = 271	
ALPHA = -0.78399979E+02	ZR = 0.33
LAST ZERO POINT I = 271	
ALPHA = -0.78499977E+02	ZR = 0.33
LAST ZERO POINT I = 271	
ALPHA = -0.78599976E+02	ZR = 0.38
LAST ZERO POINT I = 281	
ALPHA = -0.78699974E+02	ZR = 0.38
LAST ZERO POINT I = 281	
ALPHA = -0.78799973E+02	ZR = 0.38
LAST ZERO POINT I = 281	
ALPHA = -0.78899971E+02	ZR = 0.38
LAST ZERO POINT I = 281	
ALPHA = -0.78999969E+02	ZR = 0.38
LAST ZERO POINT I = 281	
ALPHA = -0.79099968E+02	ZR = 0.38
LAST ZERO POINT I = 291	
ALPHA = -0.79199966E+02	ZR = 0.43
LAST ZERO POINT I = 301	
ALPHA = -0.79299965E+02	ZR = 0.48
ALPHA = -0.79249969E+02	
LAST ZERO POINT I = 321	
ALPHA = -0.79274971E+02	ZR = 0.58
ALPHA = -0.79262474E+02	
ALPHA = -0.79256226E+02	
LAST ZERO POINT I = 341	
ALPHA = -0.79259354E+02	ZR = 0.68
ALPHA = -0.79257790E+02	
ALPHA = -0.79257011E+02	
ALPHA = -0.79256622E+02	
LAST ZERO POINT I = 351	
ALPHA = -0.79256821E+02	ZR = 0.73
LAST ZERO POINT I = 361	
ALPHA = -0.79256920E+02	
ALPHA = -0.79256874E+02	
MATCH1 = 251	
ALPHA = -0.79256874E+02	RATIO - 1.0 = -0.180399E-02

NUCLEAR CHARGE = 13.0 Z = 1.0 DIPOLE POLARIZIBILITY = 0.0000

#### SEMI-EMPIRICAL RADIAL WAVE FUNCTION

N = 1 L = 0 ENERGY (ATOM. UNITS) = -0.7925687E+02

DEBYE LENGTH = 0.100000E+01

ATDIM = 0.000000E+00

0.00000	0.00000E+00	0.03500	0.20933E+01	0.22500	0.11238E+0
0.00050	0.46877E-01	0.03900	0.22139E+01	0.25000	0.90107E+0
0.00100	0.93146E-01	0.04300	0.23167E+01	0.27500	0.71534E+0
0.00150	0.13881E+00	0.04700	0.24034E+01	0.30000	0.56325E+0
0.00200	0.18389E+00	0.05100	0.24751E+01	0.32500	0.44045E+0
0.00250	0.22837E+00	0.05500	0.25333E+01	0.35000	0.34240E+0
0.00300	0.27226E+00	0.05900	0.25791E+01	0.37500	0.26483E+0
0.00350	0.31558E+00	0.06300	0.26137E+01	0.40000	0.20394E+0
0.00400	0.35833E+00	0.06700	0.26380E+01	0.42500	0.15644E+0
0.00450	0.40051E+00	0.07100	0.26531E+01	0.45000	0.11959E+0
0.00500	0.44212E+00	0.07500	0.26597E+01	0.50000	0.69270E-0
0.00600	0.52369E+00	0.08000	0.26574E+01	0.55000	0.39729E-0
0.00700	0.60307E+00	0.08500	0.26448E+01	0.60000	0.22603E-0
0.00800	0.68031E+00	0.09000	0.26231E+01	0.65000	0.12774E-0
0.00900	0.75545E+00	0.09500	0.25935E+01	0.70000	0.71793E-0
0.01000	0.82853E+00	0.10000	0.25572E+01	0.80000	0.22370E-0
0.01100	0.89960E+00	0.10500	0.25151E+01	0.90000	0.68658E-0
0.01200	0.96869E+00	0.11000	0.24680E+01	1.00000	0.20818E-0
0.01300	0.10358E+01	0.11500	0.24169E+01	1.10000	0.62524E-0
0.01400	0.11011E+01	0.12000	0.23623E+01	1.20000	0.18637E-0
0.01500	0.11645E+01	0.12500	0.23050E+01	1.40000	0.16268E-0
0.01700	0.12858E+01	0.13500	0.21842E+01	1.60000	0.13944E-0
0.01900	0.14001E+01	0.14500	0.20585E+01	1.80000	0.11790E-0
0.02100	0.15076E+01	0.15500	0.19309E+01	2.00000	0.98670E-0
0.02300	0.16087E+01	0.16500	0.18037E+01	2.20000	0.81929E-1
0.02500	0.17036E+01	0.17500	0.16787E+01	2.40000	0.67618E-1
0.02700	0.17925E+01	0.18500	0.15574E+01	2.60000	0.55542E-1
0.02900	0.18757E+01	0.19500	0.14406E+01	2.80000	0.45448E-1
0.03100	0.19534E+01	0.20500	0.13292E+01	3.00000	0.37075E-1
0.03300	0.20259E+01	0.21500	0.12235E+01	3.20000	0.30067E-1

EIGVAL	ENERGY	INTEGRAL	XSECT (DF/DE)
-0.792569E+02	0.100000E+03	0.735737E-02	0.148477E-02
-0.792569E+02	0.500000E+02	0.110105E-01	0.268212E-02
-0.792569E+02	0.300000E+02	0.132855E-01	0.353044E-02
-0.792569E+02	0.200000E+02	0.146585E-01	0.406986E-02
-0.792569E+02	0.150000E+02	0.154090E-01	0.437135E-02
-0.792569E+02	0.120000E+02	0.158819E-01	0.456345E-02
-0.792569E+02	0.100000E+02	0.162093E-01	0.469780E-02
-0.792569E+02	0.500000E+01	0.170761E-01	0.505896E-02

-0.792569E+02	0.200000E+01	0.176328E-01	0.529522E-02
-0.792569E+02	0.100000E+01	0.179889E-01	0.547693E-02
-0.792569E+02	0.500000E+00	0.187920E-01	0.595815E-02
-0.792569E+02	0.200000E+00	0.210821E-01	0.748465E-02
-0.792569E+02	0.100000E+00	0.253847E-01	0.108446E-01
-0.792569E+02	0.500000E-01	0.328018E-01	0.181021E-01
-0.792569E+02	0.400000E-01	0.343316E-01	0.198288E-01
-0.792569E+02	0.300000E-01	0.329822E-01	0.182995E-01
-0.792569E+02	0.200000E-01	0.250204E-01	0.105303E-01
-0.792569E+02	0.100000E-01	0.127382E-01	0.272924E-02

**LISTING OF SAMPLE COMPUTER COPIES:  
FFNEW.FOR; DIFF.FOR; SIMP.FOR; WAVEF.FOR.**

```

0      PROGRAM FFNEW
C
C      Calculates photoabsorption cross sections for continuum states in
C      the DFT potential
C
COMMON U(1751),FU(1751),FV(1751),FKL(10,1751),AKL(10),
#    BFKL(10),
1    Y(1751),QR(851),Q(851),P(3,851),ENR(2),Z,STEP,ABC,EN(3),
2    LFKL(10),ICHECK(10)
COMMON/CC2/ LPOT,IORT,AMPL
COMMON /SCREEN/ GRID(851),YGRID(851)
DIMENSION ENRG(6) ,R(840),RVR(840)

C      Sum of 1>1 matrix element is ffosc
C      FFIN contains input info for continuum states etc
C      POIB contains the DFT potential
C      NUMERICAL DERIVATIVE of potential is used in matrix element
C      FFOUT contains program output of f-f cross section
C      FFOSC is osc.strength in at.unit
C
C
c      OPEN(UNIT=005,FILE='FFIN.DAT',STATUS='OLD')
c      OPEN(UNIT=009,FILE='POIB.DAT',STATUS='OLD')
c      OPEN(UNIT=006,FILE='FFOUT.DAT',STATUS='NEW')
c
      READ (5,13) ICHECK
13 FORMAT (10I1)
      READ(5,40)STEP,STEP1,ZZ
      WRITE(06,4001)
4001 FORMAT(8X,'STEP',8X,'STEP1')
      WRITE(06,4000)STEP,STEP1,ZZ
4000 FORMAT(1X,3E13.6)
40 FORMAT(3E13.6)
      WRITE(6,2050)
2050 FORMAT(//,' USING THE DFT/INPUT POTENTIAL',//)
      A=6450.0*STEP1
      Z=1.0
      IORT=0
      U(1)=0.0
      LPOT=0
      H=STEP
      J=1
      K=50
108 DO 109 I=J,K
      U(I+1)=U(J)+(I-J+1)*H
109 CONTINUE
      IF (K-250) 110,111,2000
110 H=2*STEP
      J=51
      K=250
      GO TO 108
111 H=10*STEP
      J=251
      K=1750
      GO TO 108
2000 CONTINUE

```

```

10 FORMAT (1E13.6)
C
C      VREAD reads in r and rV(r) vectors
C
C      CALL VREAD(R,RVR)
C
C      fill GRID and YGRID for interpolation
C
DO 20 I=1,840
  GRID(I)=R(I)
20 YGRID(I)=RVR(I)
  DO 21 I=841,851
    GRID(I)=0.0
21 YGRID(I)=0.0
  DO 22 I=1,851
    Q(I)=U(I)
22 CALL WAVEF(1.0,STEP,QR,Q)
  DO 23 I=1,851
    GRID(I)=U(I)
23 Y(I)=QR(I)
  DO 2  I=851,1751
2  Y(I)=0.0
C
C      Ein is the incident electron energy,Eout the emitted energy in at.unit
C
SUML=0.0
17 READ (5,10)EIN
  OMEGA =14.80
  EOUT=EIN + OMEGA
  DO 14 LL=0,35
    LLP1 = LL+1
    CALL DIFF(LL,EIN,1)
    CALL DIFF(LLP1,EOUT,2)
    QR(1)=0.
    QR(2)=0.
    QR(851)=0.
    DO 100 I=3,850
      YDA = Y(I)/U(I)-Y(I-1)/U(I-1)
      YDB = Y(I+1)/U(I+1)-Y(I-1)/U(I-1)
      XDA = U(I)-U(I-1)
      XDB = U(I+1)-U(I-1)
      XI2 = (YDA*XDB-YDB*XDA)/(XDA*XDB*(XDA-XDB))
      XI1 = YDA/XDA - XI2*XDA
      QR(I) = XI1 + 2.*XDA*XI2
100 QR(I)=QR(I)*FKL(1,I)*FKL(2,I)
    CALL SIMP(X)
    A=X**2/OMEGA**3
    XLLP1=LLP1
    XLL = LL
    FFOSC=(16.0*XLLP1*A)/3.0
C
C      Sum over all 1 values
C
SUML =SUML+FFOSC
14 CONTINUE
  WRITE (6,51)
51 FORMAT(//,5X,'OMEGA',5X,'EIN',10X,'EOUT',10X,'+SUML')

```

```
      WRITE(6,52)OMEGA,EIN,EOUT,SUML
52  FORMAT(/,4E13.6)
      GO TO 17
      END
C
C
      SUBROUTINE VREAD(R,RVR)
      DIMENSION R(840), RVR(840)
C
C      READS DFT EFFECTIVE POTENTIAL RVR
C
      READ(9,11)(R(I),I=1,840)
11   FORMAT(6E13.6)
      READ(9,11)(RVR(I),I=1,840)
      WRITE(06,33)((R(I),RVR(I)),I=1,100,4)
33   FORMAT(1X,E13.6,2X,E13.6)
      WRITE(6,106)
106  FORMAT(///)
      RETURN
C
C
      END
```

```

SUBROUTINE DIFF(L,ENRG,IFKL)
C
C Numerical Solution Of Continuum States of Schrodinger Eq.
C
COMMON U(1751),FU(1751),FV(1751),FKL(10,1751),AFKL(10),BFKL(10),
1 Y(1751),QR(851),Q(851),P(3,851),ENR(2),Z,STEP,ABC,EN(3),
2 LFKL(10),ICHECK(10)
COMMON/CC2/ LPOT,IORT,AMPL
DIMENSION FAC(150)
REAL*8 BL,ENER,UA,UB,UC,AU,BU,CU,DU,B1,B2,B3,B4,B5,B6
REAL*8 BUG,CUG,DUG
LFKL(IFKL)=L
IF (L.LT.0) RETURN
ENER=ENRG*1.0D+00
AL=L
IF (ENER.LT.0.0) GO TO 1325
IF (LPOT.EQ.0.AND.ENER.LT.1D-03) GO TO 6010
ENER=ENER/Z**2
ST=1.0
J1=0
Q0=0.0
Q1=0.0
IF (L.LT.10) GO TO 6006
IF (IORT.NE.0) WRITE (6,6013) L
6013 FORMAT (////,5X,14HWARNING L = ,I3,/5X,37HFKL FOR L.GT.9 ARE NOT
1 ORTHOGONALIZED,///)
IORT=0
Y1=Y(17)-Y(1)
Y2=Y(33)-Y(1)
Z1=(4*Y1-Y2)/(32*STEP)
Z2=(Y2-2*Y1)/(512*STEP**2)
K=51
GO TO 6007
6006 K=11
Y1=Y(6)-Y(1)
Y2=Y(11)-Y(1)
Z1=(4*Y1-Y2)/(10*STEP)
Z2=(Y2-2*Y1)/(50*STEP**2)
IF (IORT.EQ.0) GO TO 6007
A=Q(6)/U(6)**(L+1)
B=Q(11)/U(11)**(L+1)
Q0=2*A-B
IF (Q0.LT.0.0) Q0=0.0
Q1=(B-Q0)/U(11)
BB=Y(1)*ST/(AL+1.0)
CC=(-2*Y(1)*BB-2*Z1*ST-2*ENER*ST)/(4*AL+6.0)
CC=CC+Q0/(4*AL+6.0)
DD=(-2*Y(1)*CC-2*Z1*BB-2*Z2*ST-2*ENER*BB)/(6*AL+12.0)
DD=DD+Q1/(6*AL+12.0)
FU(1)=0.0
B=1.0
1246 DO 1245 I=2,K
A=U(I)*B
IF (L.EQ.0) GO TO 1245
DO 6001 J=1,L

```

```

A=A*U(I)
IF (ABS(A).LT.1E-20) A=0.0
6001 CONTINUE
1245 FU(I)=(ST+BB*U(I)+CC*U(I)**2+DD*U(I)**3)*A
BL=L*(L+1)
IF (ABS(FU(K)).LT.1E-20) GO TO 6008
IF (20-K) 302,302,6009
6008 J1=J1+1
B=10*B
GO TO 1246
6009 H=STEP**2
K=50
K1=10
K2=11
K3=12
300 BU=1.0-(BL/U(K1)**2-2.000*Y(K1)/U(K1)-2.0*ENR)*H/12.0
CU=1.0-(BL/U(K2)**2-2.000*Y(K2)/U(K2)-2.0*ENR)*H/12.0
DU=1.0-(BL/U(K3)**2-2.000*Y(K3)/U(K3)-2.0*ENR)*H/12.0
AU=12.0-10.0*CU
UA=FU(K1)*1.000
UB=FU(K2)*1.000
BUG=100*Q(K1)
CUG=100*Q(K2)
DUG=100*Q(K3)
DO 301 I=K2,K
UC=(AU*UB-BU*UA)/DU
IF (IORT.EQ.0 ) GO TO 6012
IF (I.GT.850) GO TO 6012
UC=UC+(BUG+10*CUG+DUG)*H/12.0
6012 FU(I+1)=UC
IF (DABS(UC).LT.1E+25) GO TO 3050
J1=J1-10
UB=UB*1D-10
UC=UC*1D-10
JM=I+1
5000 FU(JM)=FU(JM)*1E-10
IF (JM.EQ.2) GO TO 3050
IF (ABS(FU(JM)).LT.1E-20) GO TO 5002
JM=JM-1
GO TO 5000
5002 DO 5003 KM=2,JM
5003 FU(KM)=0.0
3050 BU=CU
CU=DU
DU=1.0-(BL/U(I+2)**2-2.000*Y(I+2)/U(I+2)-2.0*ENR)*H/12.0
AU=12.0-10.0*CU
UA=UB
IF (IORT.EQ.0.OR.I.GT.849) GO TO 301
BUG=BUG
CUG=CUG
DUG=100*Q(I+2)
301 UB=UC
IF (K-250) 302,303,304
302 H=4*STEP**2
K1=49
K2=51
K3=52

```

```

K=250
GO TO 300
303 H=100*STEP**2
K1=246
K2=251
K3=252
K=1749
GO TO 300
304 FU(1751)=(AU*FU(1750)-BU*UA)/DU
J=0
DO 3049 I=10,105
IF ((FU(I).LT.0.0.AND.FU(I+1).GT.0.0).OR.(FU(I).GT.0.0.AND.
1 FU(I+1).LT.0.0)) J=J+1
3049 CONTINUE
K=1
MAMPL=0
DO 305 I=1006,1748
IF ((FU(I).LT.0.0.AND.FU(I+1).GT.0.0).OR.(FU(I).GT.0.0.AND.
1 FU(I+1).LT.0.0)) GO TO 306
GO TO 999
306 B1=FU(I-2)*1.0D+00
B2=FU(I-1)-B1
B3=(FU(I)-B1-2*B2)/2.0
B4=(FU(I+1)-B1-3*B2-6*B3)/6.0
B5=(FU(I+2)-B1-4*B2-12*B3-24*B4)/24.0
B6=(FU(I+3)-B1-5*B2-20*B3-60*B4-120*B5)/120.0
B=U(I)+10*STEP*ABS(FU(I))/(ABS(FU(I))+ABS(FU(I+1)))
D1=B- U(I-2)
D2=B- U(I-1)
D3=B- U(I)
D4=B- U(I+1)
D5=B- U(I+2)
D6=B- U(I+3)
C=0.1/SIPEP
A=C *B2+C*C*B3*(D1+D2)+C**3*B4*(D1*D2+D1*D3+D2*D3)+C**4 *B5*
1 (D1*D2*D3+D1*D2*D4+D1*D3*D4+D2*D3*D4)+C**5 *B6*(D1*D2*D3*D4+
2 D1*D2*D3*D5+D1*D2*D4*D5+D1*D3*D4*D5+D2*D3*D4*D5)
D=Y(I)+C *(B-U(I))*(Y(I+1)-Y(I))
C=BL/B**2+2.0*D/B+2.0*ENER
IF (C.LT.0.0) MAMPL=1
IF (C.LT.0.0) GO TO 999
C=ABS(C)
C=SORT(C)
C=SORT(C)
FAC(K)=ABS(C/(A*SORT(Z)))
IF (ICHECK(1).NE.0) WRITE (6,703) L,K,B,FAC(K)
703 FORMAT (2I5,F10.4,E20.8)
K=K+1
IF (K.EQ.71) GO TO 3040
999 CONTINUE
305 CONTINUE
3042 A=0.0
K=K-1
IF (MAMPL.EQ.1) J=0
IF (MAMPL.EQ.1.AND.K.EQ.0) WRITE (6,6011) L, ENRG
IF (K.EQ.0) GO TO 1220
DO 307 I=1,K

```

```

307 A=A+FAC(I)
B=K
A=A/B
IF (J.EQ.0) A=FAC(K)
AMPL=A
GO TO 1221
1220 WRITE (6,1222) L
AMPL=0.0
1222 FORMAT (10X,29HAMPLITUDE NOT DETERMINED L =, 15)
GO TO 1325
1221 DO 308 I=1,1750
J=1752-I
B=A*FU(J)
IF (ABS(B).GT.1E-08) GO TO 6000
B=FU(J-1)*A
IF (ABS(B).LT.1E-08) GO TO 3046
6000 CONTINUE
308 FU(J)=B
GO TO 3047
3046 DO 3048 I=1,J
3048 FU(I)=0.0
3047 CONTINUE
B=15450*STEP
A=(-BL/B**2+2*Y(1751)/B+2*ENER)*Z*Z
A=ABS(A)
A=SQRT(A)
A=SQRT(A)
A=A*FU(1751)
IF (ABS(A).GT.0.9) GO TO 1210
GO TO 1212
1210 I=1751
4001 I=I-2
IF (FU(I)/FU(1751).LT.0.71) GO TO 4000
GO TO 4001
4000 A=2.0*L POT/U(I )-BL/U(I )**2+2*ENER
A=SQRT(A)
B1=SQRT(A)*SQRT(Z)
D=0.0
J=I
4002 B=2.0*L POT/U(I+1)-BL/U(I+1)**2+2*ENER
B=SQRT(B)
C=2.0*L POT/U(I+2)-BL/U(I+2)**2+2*ENER
C=SQRT(C)
D=D+A+4*B+C
I=I+2
A=C
IF (I.LT.1751) GO TO 4002
D=D*10.0*STEP/3.0
A=B1*FU(J)
C=1.0
IF (FU(J+1) LT.FU(J)) C=-1.0
B=C*SOP'(1.0-A*A)
C=SIN(P)
D=CCS(D)
APKL(IPKL)=A*D+B*C
BKLN(IPKL)=B*D-A*C
GO TO 4003

```

```
1212 C=1.0
      IF (FU(1751).LT.FU(1750)) C=-1.0
      B=C*SQRT(1.0-A*A)
1213 AFKL(IFKL)=A
      BFKL(IFKL)=B
4003 DO 3052 I=1,1751
3052 FKL(IFKL,I)=FU(I)
      RETURN
1325 DO 1326 I=1,1751
1326 FU(I)=0.0
      A=0.0
      B=0.0
      GO TO 1213
3040 AAX=ENRG*Z**2
      IF (L.EQ.0) WRITE (6,3041) AAX
3041 FORMAT (//,10X,20HENERGY (AT. UNITS) =,E15.6/10X,97HPROGRAM MAY NO
      IT GIVE CORRECT AMPLITUDE OF CONTINUUM FUNCTIONS AT SUCH HIGH ENERG
      2Y - DECREASE STEP,//)
      GO TO 3042
6010 WRITE (6,6011) L,ENRG
6011 FORMAT (/,10X,53HWARNING - PROGRAM CANNOT COMPUTE FKL FOR SMALL EN
      ERGY/10X,4H = ,I5,10X,9HENERGY = ,E14.6)
      GO TO 1325
      END
```

```

SUBROUTINE WAVEF(Z,SIEP,Q,U)
DIMENSION Q(851),U(851),FU(1751),FV(1751)
DIMENSION NP(14),ZET(14),CLEM(14),TPL(1751)
COMMON /SCREEN/ GRID(851),YGRID(851)

C KMAX MAY BE SET EQUAL TO 14 IF NUMBER OF TERMS IN THE EXPANSION
C FOR THE RADIAL WAVE FUNCTION IS GREATER THAN 7
KMAX=7
READ (5,1) M,(NP(I),I=1,KMAX)
IF (M.GT.0) GO TO 2
1 FORMAT (15I2)
READ (5,3) (ZET(I),I=1,KMAX)
READ (5,3) (CLEM(I),I=1,KMAX)
3 FORMAT (7F10.5)
DO 23 I=1,KMAX
M=2*NP(I)
A=2*ZET(I)
B=A
IF (M.EQ.0) GO TO 24
DO 25 MF=1,M
25 A=A/MF
CLEM(I)=CLEM(I)*B**NP(I)
24 CLEM(I)=CLEM(I)*SQR(A)
23 CONTINUE
Q(1)=0.0
DO 26 I=2,851
R=U(I)/Z
C=0.0
DO 27 J=1,KMAX
IF (NP(J).EQ.0) GO TO 31
A=R*ZET(J)
IF (A.GT.23.0) GO TO 28
B=EXP(-A)
GO TO 29
28 B=0.0
29 C=C+B*R**NP(J)*CLEM(J)
27 CONTINUE
31 Q(I)=C
26 CONTINUE
RETURN
2 IF (M.EQ.2) GO TO 101
IF (M.EQ.1) GO TO 112
DO 113 I=1,851
113 FV(I)=YGRID(I)
DO 115 I=852,1751
115 FV(I)=YGRID(851)
112 CONTINUE
J=1
K=10
RMAX=6450*SIEP/Z
11 IF (M.EQ.1) READ (5,5) (FU(I),I=J,K)
IF (M.EQ.1) GO TO 110
DO 111 I=J,K
111 FU(I)=GRID(I)
110 CONTINUE
5 FORMAT (10F8.5)
IF (FU(K).LT.RMAX) GO TO 6

```

```
      WRITE (6,7)
7 FORMAT (//,10X,62HWARNING - WAVE FUNCTION EXCEEDS ALLOWED REGION -
1 INCREASE STEP)
      STOP
6 IF (K.LE.1740) GO TO 8
      WRITE (6,9)
9 FORMAT (//,10X,68HWARNING - WAVE FUNCTION GIVEN BY NUMBER OF VALUE
1S GREATER THAN 1740)
      STOP
8 IF (FU(K).GT.0.0) GO TO 10
      IN=K-10
      GO TO 12
10 J=J+10
      K=K+10
      GO TO 11
12 DO 13 I=1,IN
13 FU(I)=FU(I)*Z
      A=FU(IN)-FU(IN-1)
      DO 14 I=IN,1750
14 FU(I+1)=FU(I)+A
      IF (FU(1751) .GT. 6450*STEP) GO TO 103
      FU(1751) = 6450*STEP + 5.0
103 DO 100 I = 1, 1751
100 TPL(I) = FU(I)
      GO TO 4
101 DO 102 I = 1, 1751
102 FU(I) = TPL(I)
      4 IF (M.EQ.3) GO TO 114
      READ (5,5) (FV(I),I=1,IN)
      DO 15 I = IN, 1750
15 FV(I+1) = 0.0
114 CONTINUE
      Q(1) = 0.0
      DO 16 I = 2, 851
      DO 17 J = 1, 1751
      IF (FU(J) .GT. U(I)) GO TO 18
17 CONTINUE
18 A = FU(J+1) - FU(J - 1)
      B = FU(J) - FU(J - 1)
      C = FU(J+1) - FU(J)
      Q(I)=FV(J-1)+((FV(J)-FV(J-1))*A*(FU(J+1)-U(I))+(FV(J+1)-FV(J-1))
      1      *B*(U(I)-FU(J)))*(U(I)-FU(J-1))/(A*B*C)
16 CONTINUE
      IF (M.EQ.3) Q(1)=2*Q(2)-Q(3)
      RETURN
      END
```

```
SUBROUTINE SIMP(THETA)
COMMON U(1751),FU(1751),FV(1751),FKL(10,1751),AFKL(10),BFKL(10),
1   Y(1751),QR(851),Q(851),P(3,851),ENR(2),Z,STEP,ABC,EN(3),
2   LFKL(10),ICHECK(10)
H=STEP
THETA=H*(4.0*QR(2)+QR(3))/3.0
JA=3
KA=49
801 DO 802 IA=JA,KA,2
802 THETA=THETA+H*(QR(IA)+4*QR(IA+1)+QR(IA+2))/3.0
IF (KA-249) 803,804,805
803 H=2*STEP
JA=51
KA=249
GO TO 801
804 H=10*STEP
JA=251
KA=849
GO TO 801
805 RETURN
END
```